Electronic Supplementary Material (ESI) for Green Chemistry.
This journal is © The Royal Society of Chemistry 2015

Supporting information for

Multifunctional β-amino alcohols as bio-based amine curing agents for the isocyanate- and phosgene-free synthesis of 100 % bio-based polyhydroxyurethane thermosets

H. Blattmann[a] and R. Mülhaupt[a,b]

[a.] *Freiburg Materials Research Center (FMF) and Institute for Macromolecular Chemistry, Stefan-Meier Strasse 31, D-79104 Freiburg, Germany.*
[b.] *E-mail: rolfmuelhaupt@web.de*

Table of contents

1. NMR spectra of prepared amino alcohols and cyclic carbonates
2. MS spectrum of L-AA after recrystallization from acetonitrile.
3. IR spectra of prepared amino alcohols and NIPU samples
4. DSC curves of prepared amino alcohols
5. Gelation and pot life time of NIPU resins
6. Shear-dependent viscosity of NIPU resins
7. Swelling degrees in water and toluene
8. DMA curves of NIPU samples
9. TGA curves of prepared amino alcohols and NIPU samples

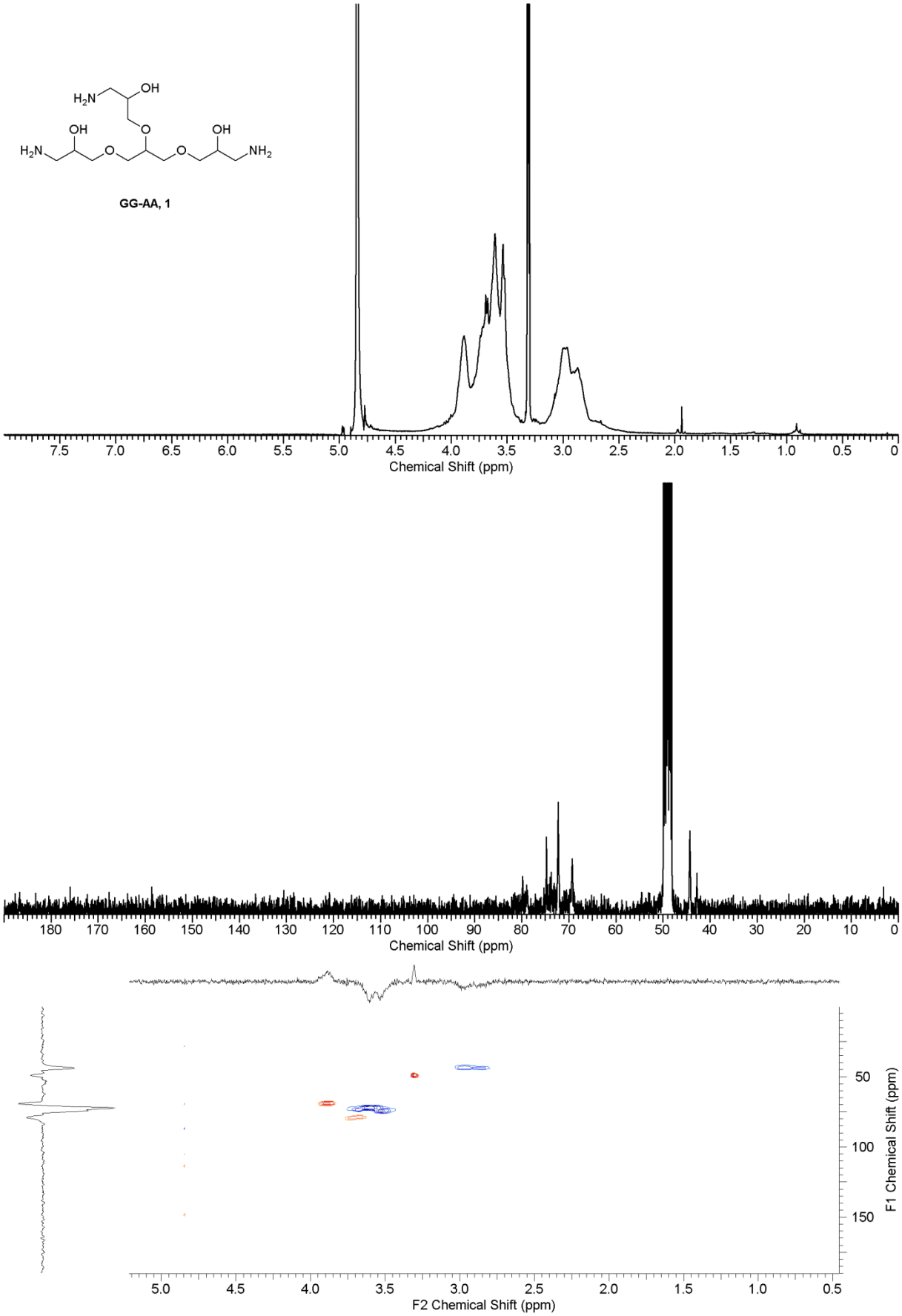

Fig. S 1 ^{1}H-NMR spectrum in MeOD-d_4 (top), ^{13}C-NMR spectrum MeOD-d_4 (center), and HSQC NMR spectrum (bottom) of GG-AA (**1**).

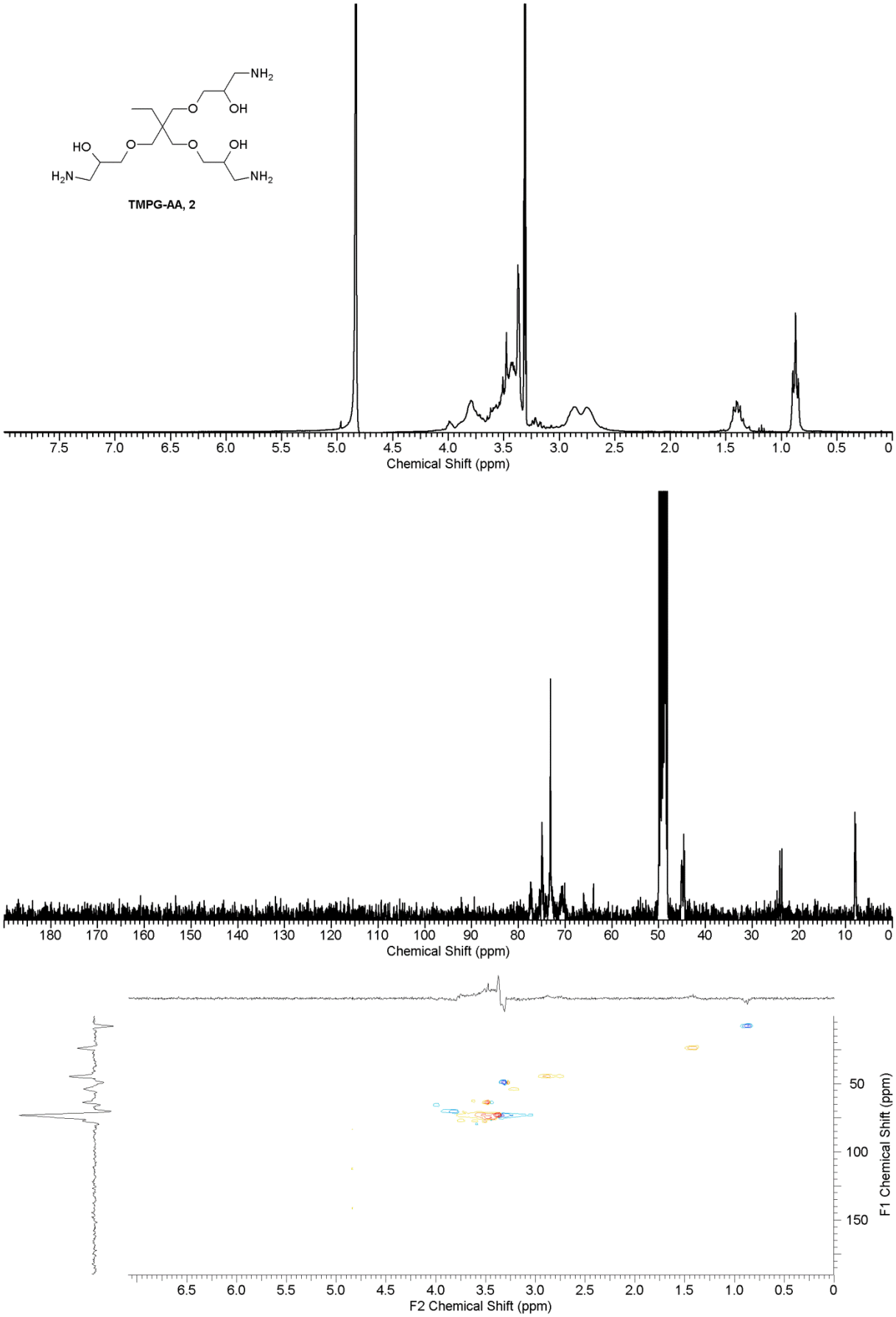

Fig. S 2 ^{1}H-NMR spectrum in MeOD-d_4 (top), ^{13}C-NMR spectrum MeOD-d_4 (center), and HSQC NMR spectrum (bottom) of TMPG-AA (**2**).

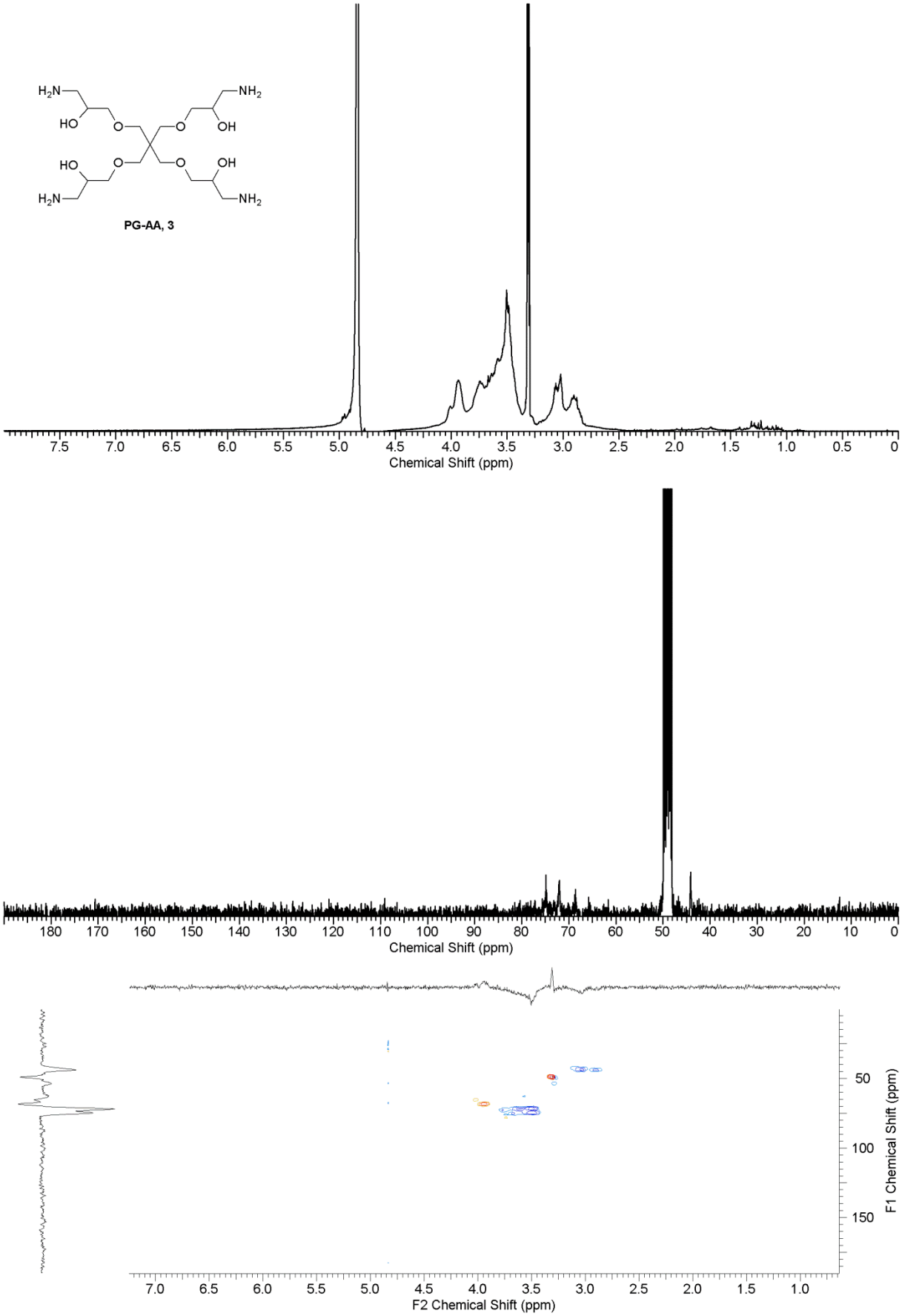

Fig. S 3 ^{1}H-NMR spectrum in MeOD-d_4 (top), ^{13}C-NMR spectrum MeOD-d_4 (center), and HSQC NMR spectrum (bottom) of PG-AA (**3**).

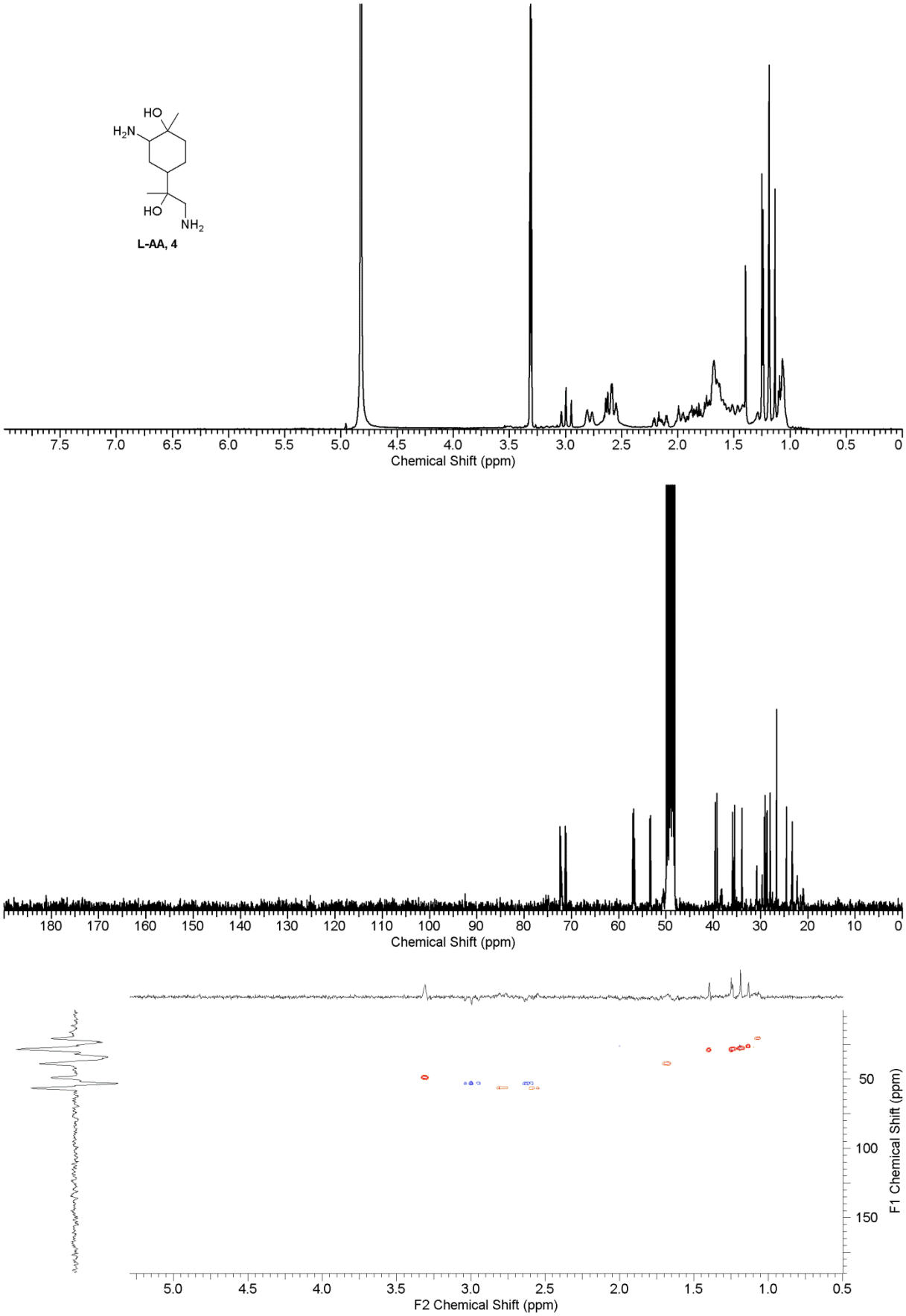

Fig. S 4 ^{1}H-NMR spectrum in MeOD-d_4 (top), ^{13}C-NMR spectrum MeOD-d_4 (center), and HSQC NMR spectrum (bottom) of crude L-AA (**4**).

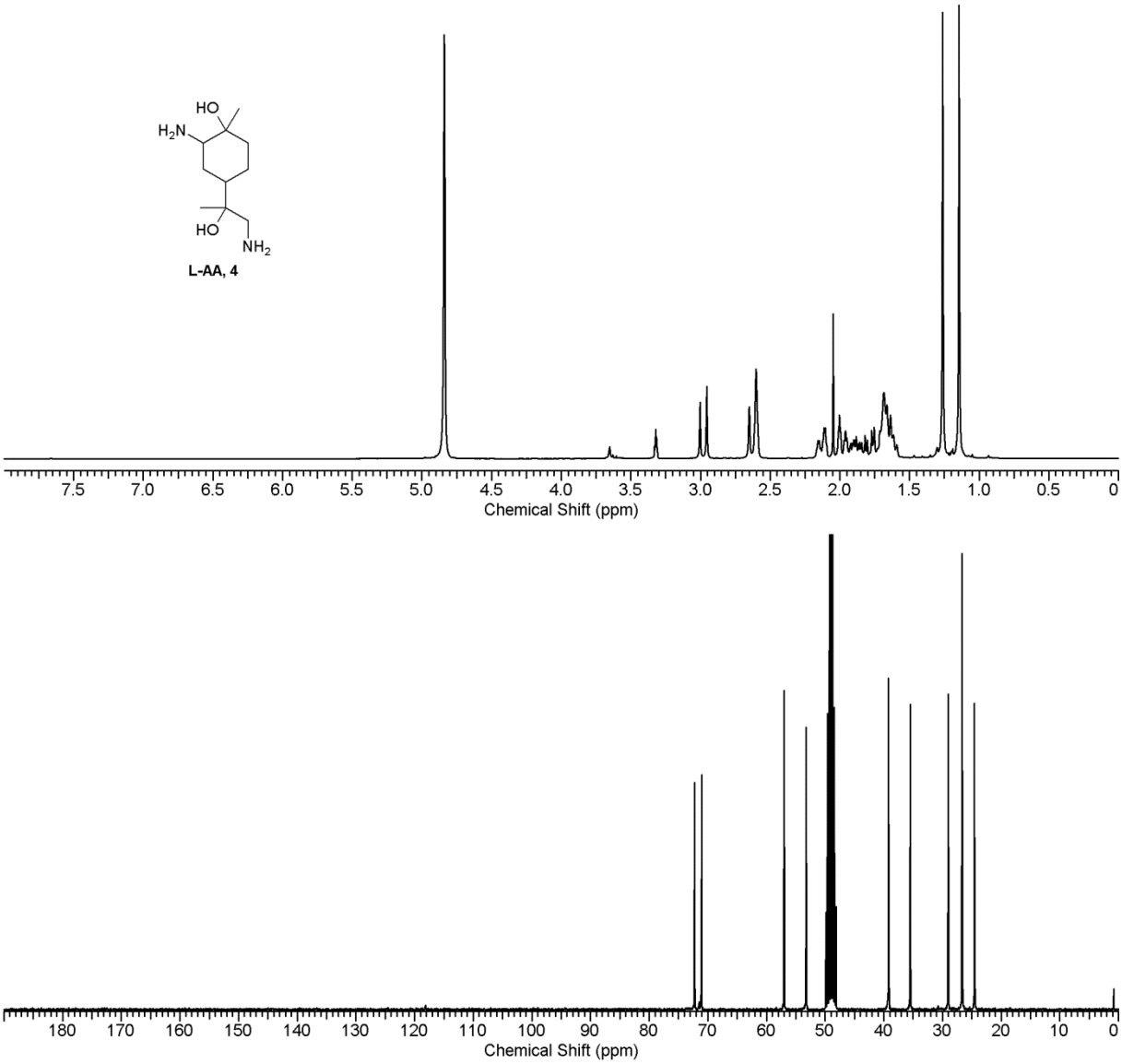

Fig. S 5 ^{1}H-NMR spectrum in MeOD-d_4 (top) and ^{13}C-NMR spectrum MeOD-d_4 (bottom) of L-AA (**4**) after recrystallization from acetonitrile.

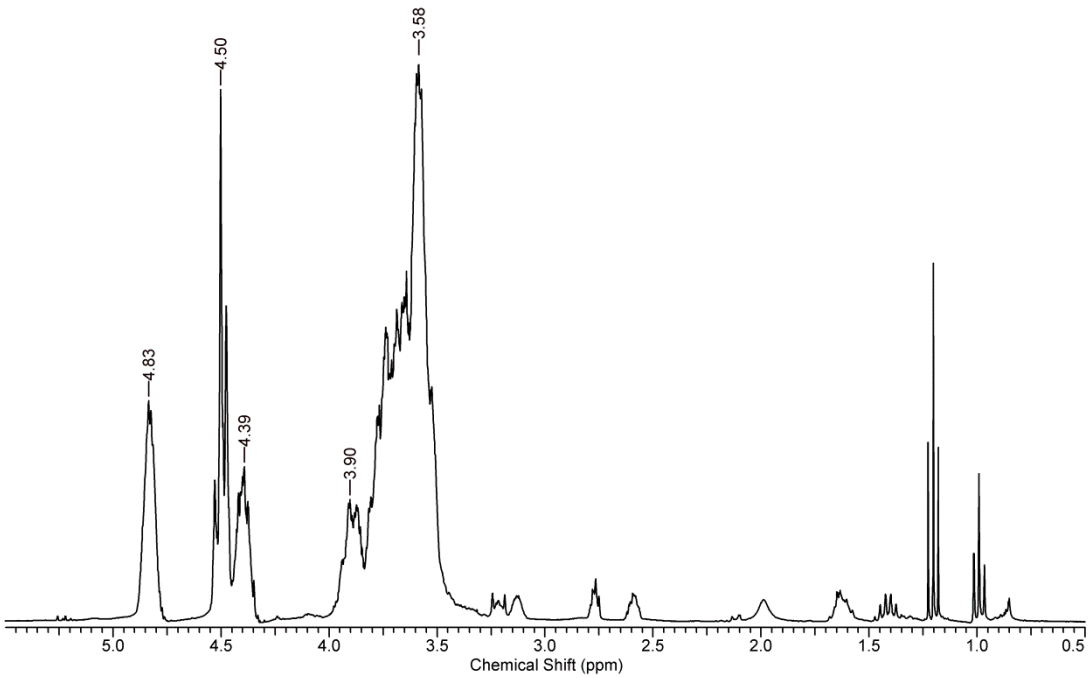

Fig. S 6 ^{1}H-NMR spectrum in $CDCl_3$ of GGC (**5**).

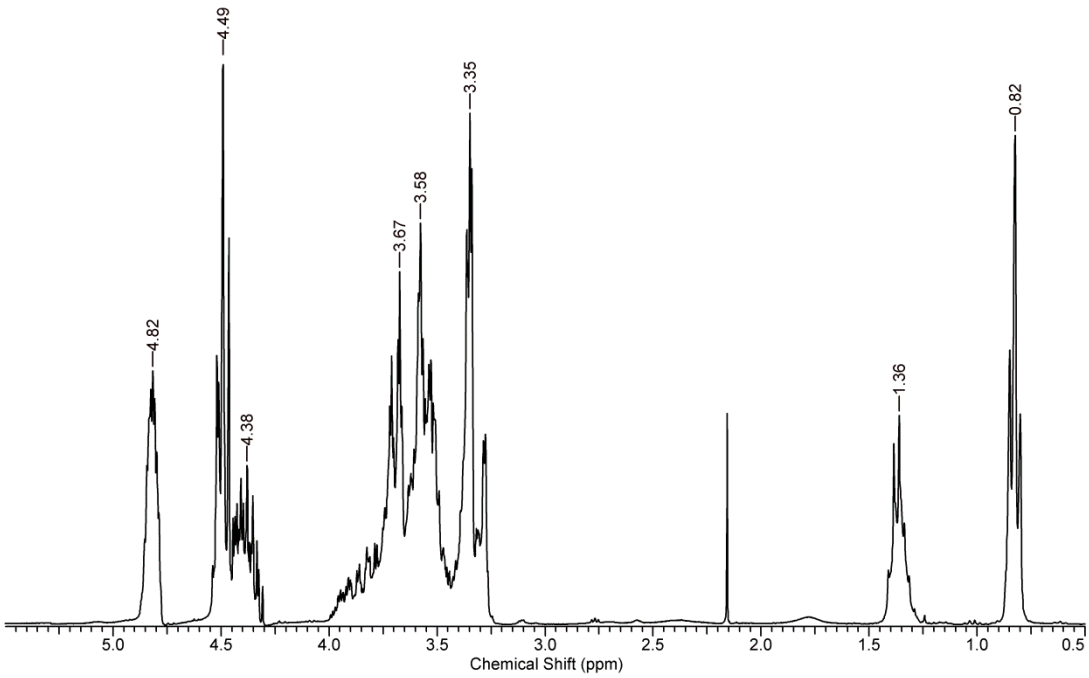

Fig. S 7 ^{1}H-NMR spectrum in $CDCl_3$ of TMPGC (**6**).

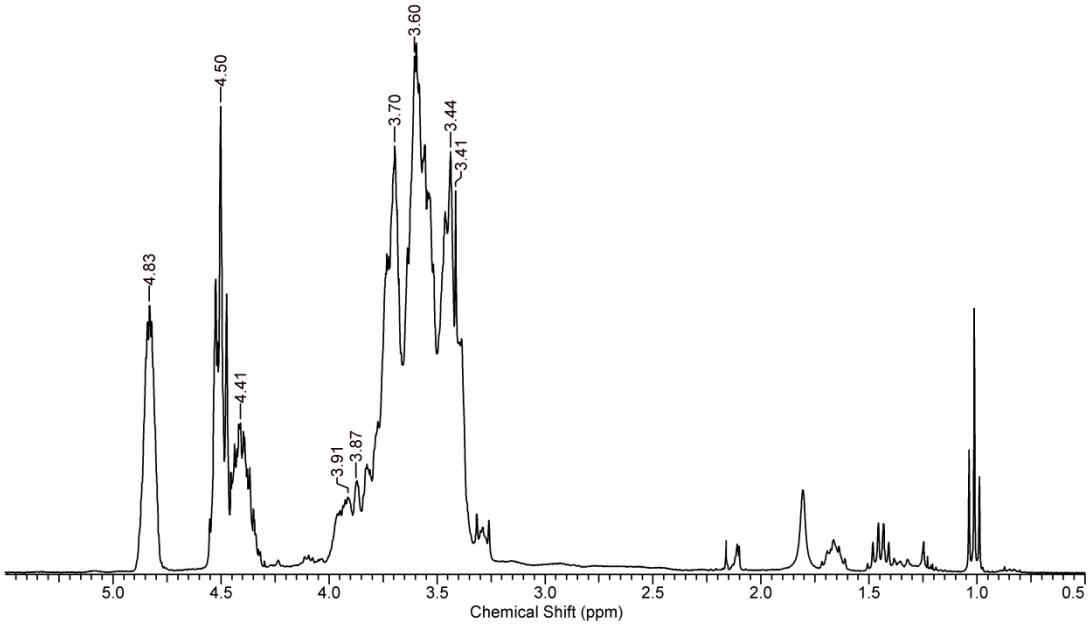

Fig. S 8 ^{1}H-NMR spectrum in $CDCl_3$ of PGC (**7**).

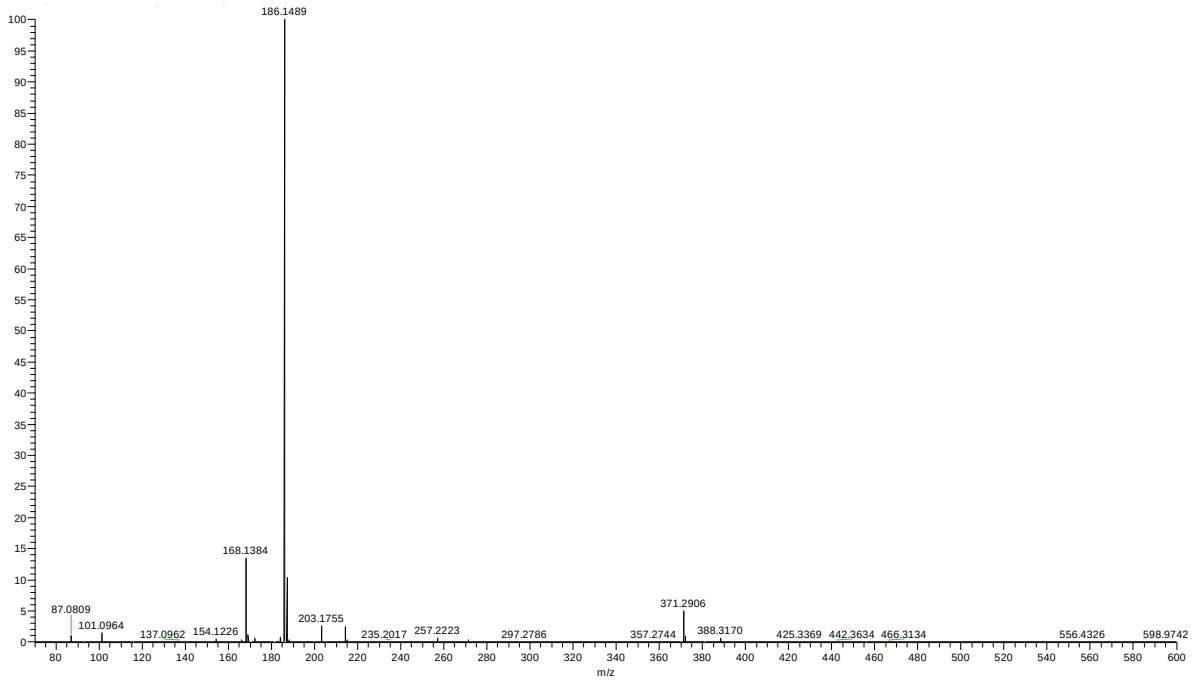

Fig. S 9 MS spectrum (dir-HR-pos, +100 V, APCI, MeOH) of L-AA (4) after recrystallization from acetonitrile.

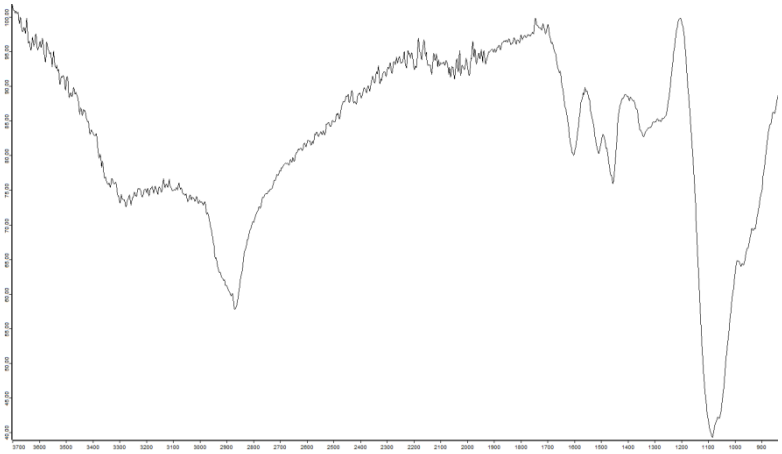

Fig. S 10 IR spectrum of GG-AA (**1**).

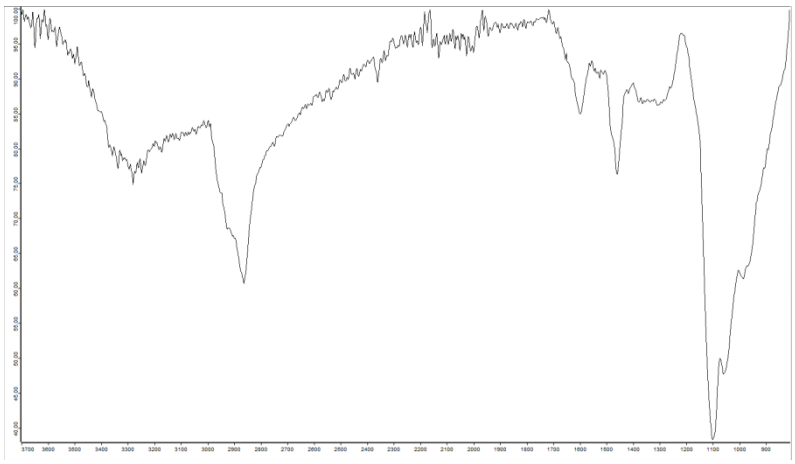

Fig. S 11 IR spectrum of TMPG-AA (**2**).

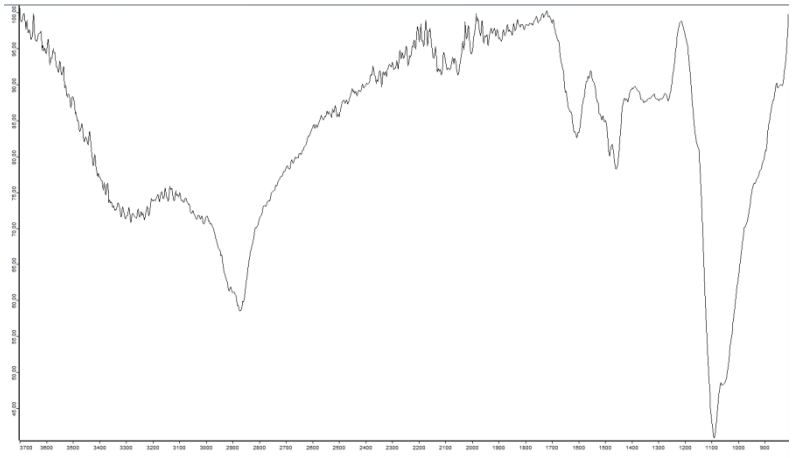

Fig. S 12 IR spectrum of PG-AA (**3**).

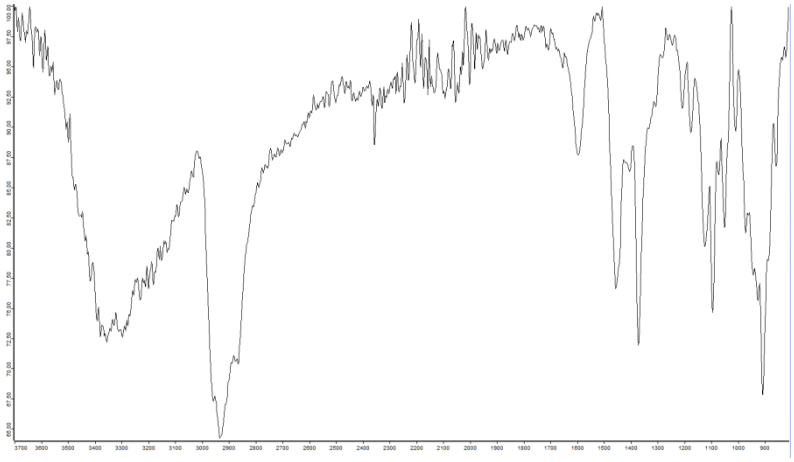

Fig. S 13 IR spectrum of L-AA (**4**).

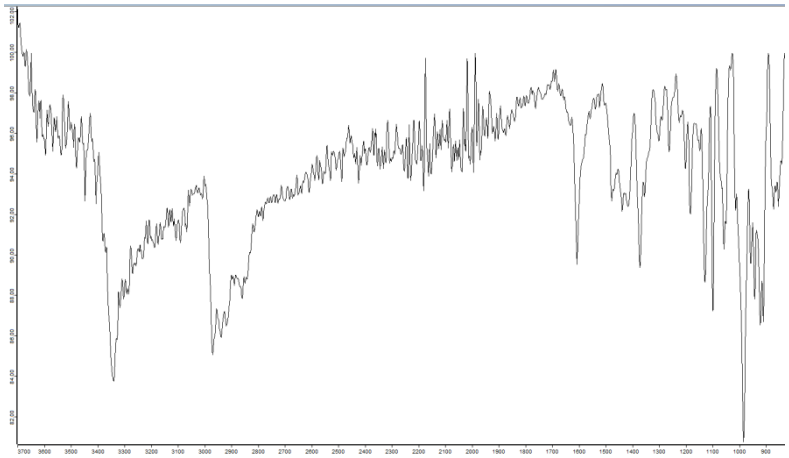

Fig. S 14 IR spectrum of L-AA (**4**) after recrystallization from acetonitrile.

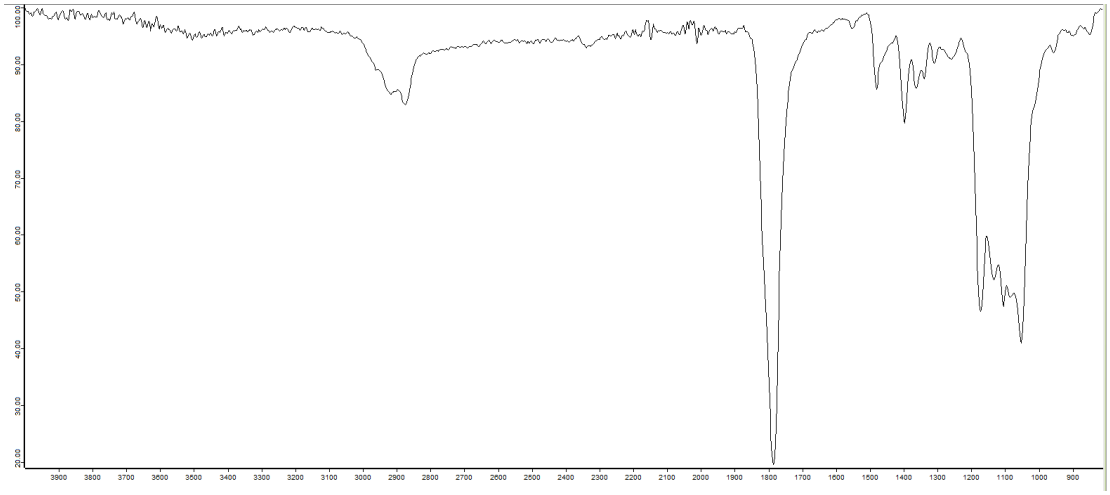

Fig. S 15 IR spectrum of GGC (**5**).

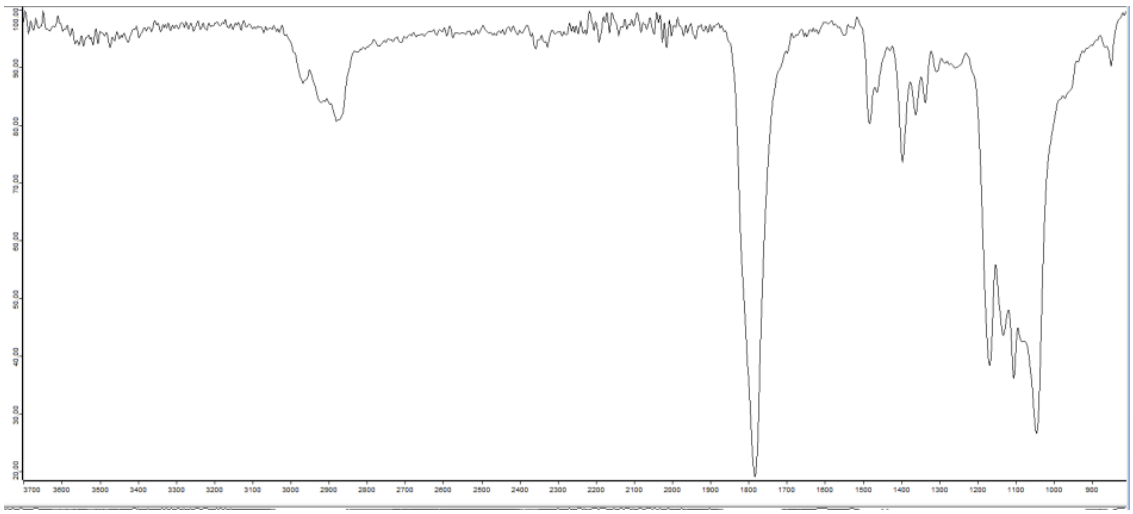

Fig. S 16 IR spectrum of TMPGC (**6**).

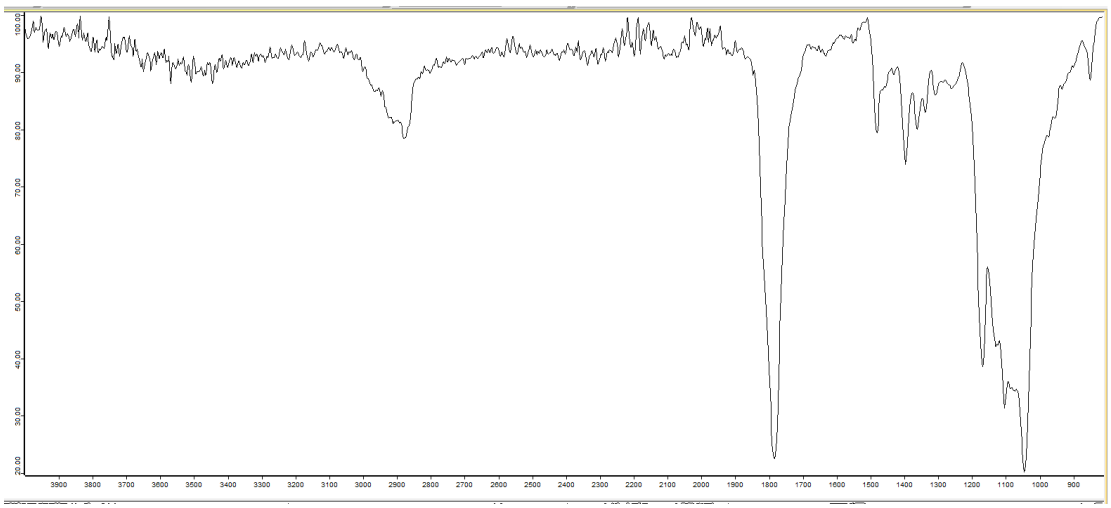

Fig. S 17 IR spectrum of PGC (**7**).

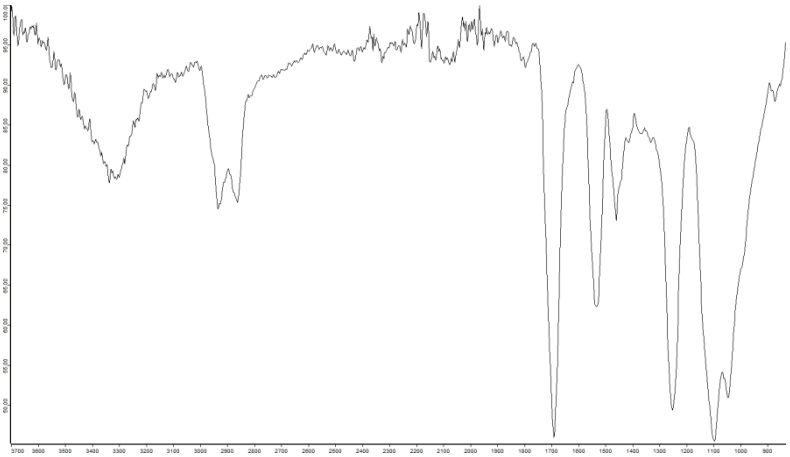

Fig. S 18 IR spectrum of NIPU sample TMPGC+HMDA (cured at 80 °C for 14 h and post-cured 4 h at 100 °C).

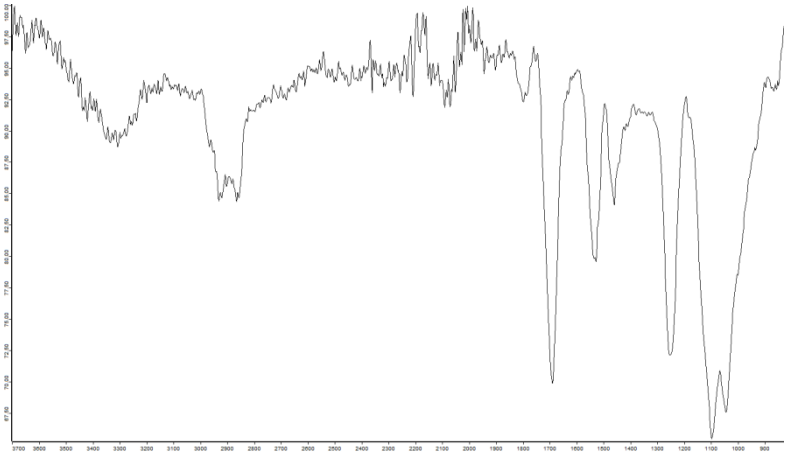

Fig. S 19 IR spectrum of NIPU sample TMPGC+HMDA+25 wt.-% GG-AA (cured at 80 °C for 14 h and post-cured 4 h at 100 °C).

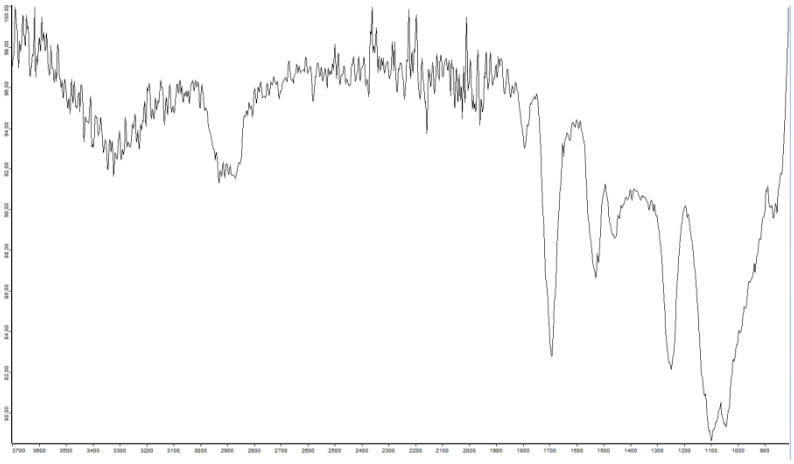

Fig. S 20 IR spectrum of NIPU sample TMPGC+HMDA+50 wt.-% GG-AA (cured at 80 °C for 14 h and post-cured 4 h at 100 °C).

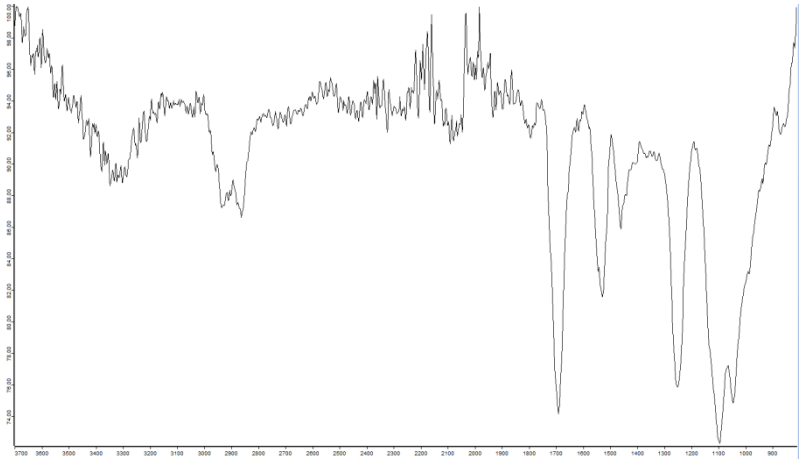

Fig. S 21 IR spectrum of NIPU sample TMPGC+HMDA+25 wt.-% TMPG-AA (cured at 80 °C for 14 h and post-cured 4 h at 100 °C).

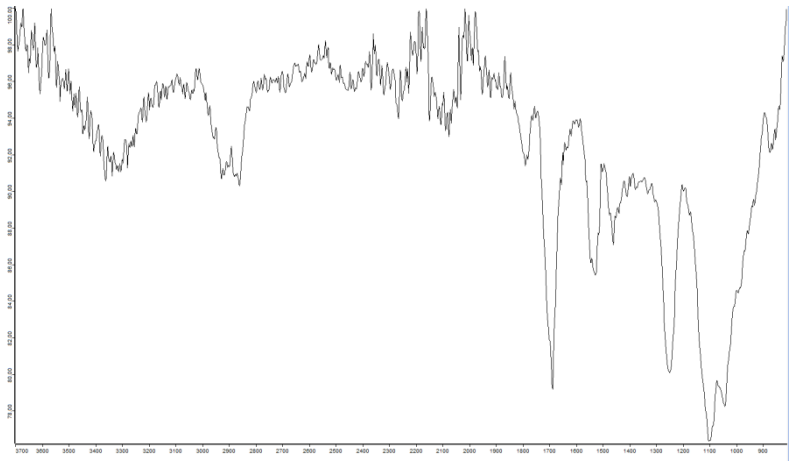

Fig. S 22 IR spectrum of NIPU sample TMPGC+HMDA+50 wt.-% TMPG-AA (cured at 80 °C for 14 h and post-cured 4 h at 100 °C).

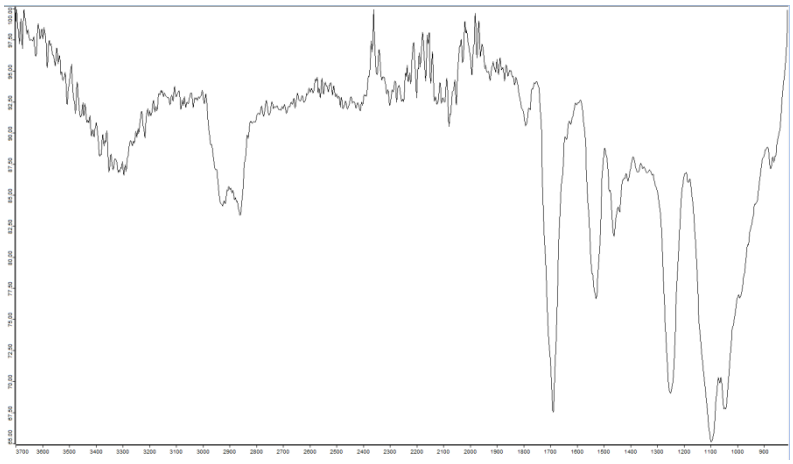

Fig. S 23 IR spectrum of NIPU sample TMPGC+HMDA+25 wt.-% PG-AA (cured at 80 °C for 14 h and post-cured 4 h at 100 °C).

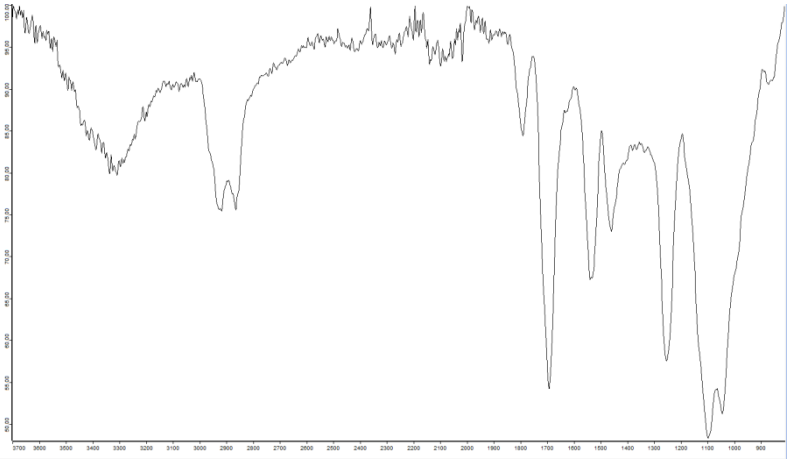

Fig. S 24 IR spectrum of NIPU sample TMPGC+HMDA+50 wt.-% PG-AA (cured at 80 °C for 14 h and post-cured 4 h at 100 °C).

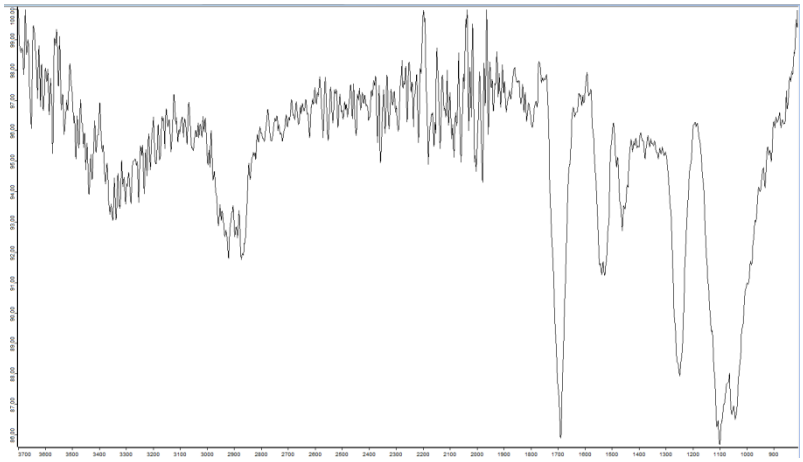

Fig. S 25 IR spectrum of NIPU sample TMPGC+HMDA+25 wt.-% L-AA (cured at 80 °C for 14 h and post-cured 4 h at 100 °C).

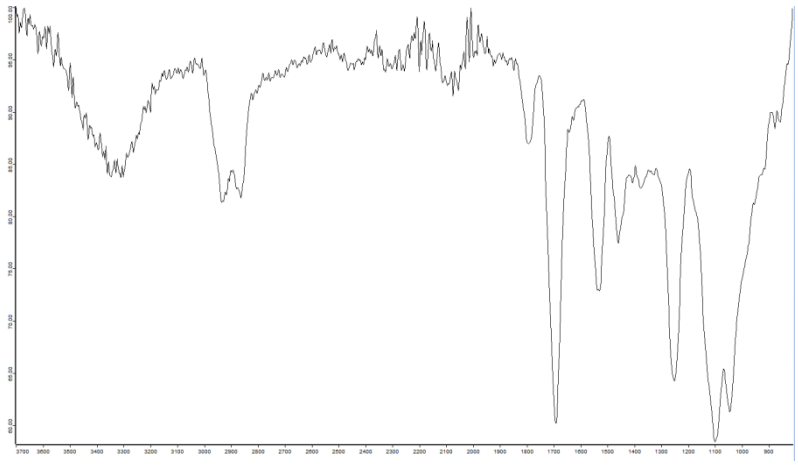

Fig. S 26 IR spectrum of NIPU sample TMPGC+HMDA+50 wt.-% L-AA (cured at 80 °C for 14 h and post-cured 4 h at 100 °C).

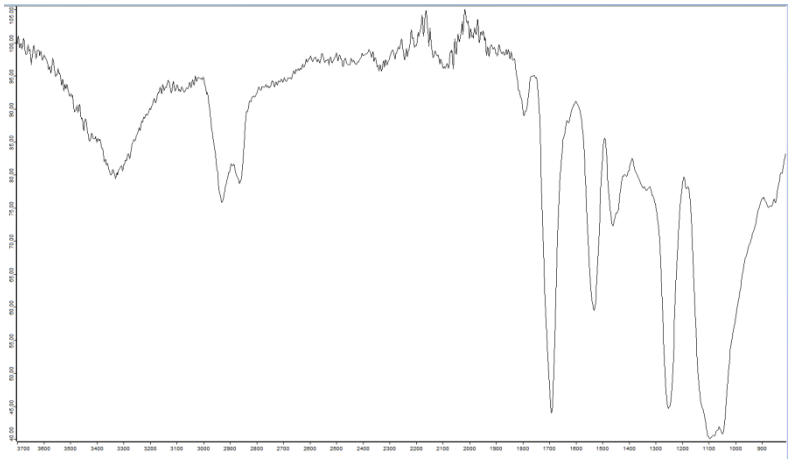

Fig. S 27 IR spectrum of NIPU sample GGC+HMDA (cured at 80 °C for 14 h and post-cured 4 h at 100 °C).

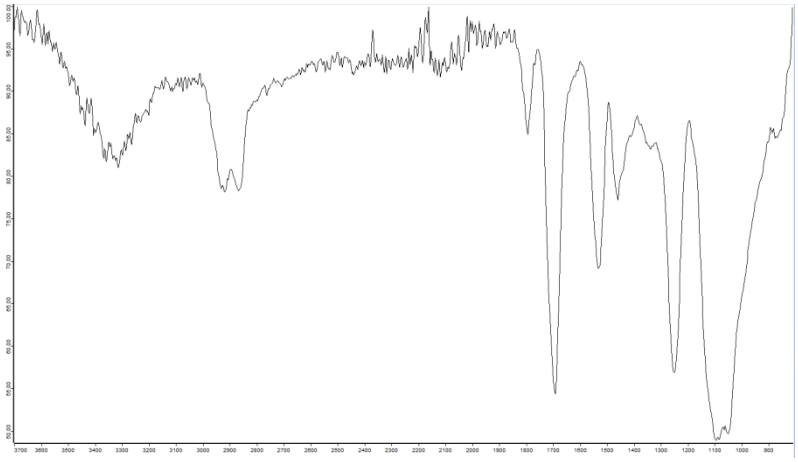

Fig. S 28 IR spectrum of NIPU sample GGC+HMDA+50 wt.-% TMPG-AA (cured at 80 °C for 14 h and post-cured 4 h at 100 °C).

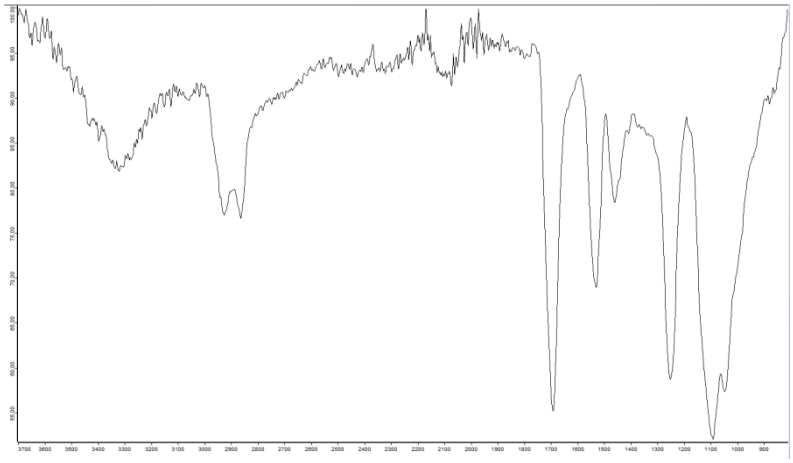

Fig. S 29 IR spectrum of NIPU sample PGC+HMDA (cured at 80 °C for 14 h and post-cured 4 h at 100 °C).

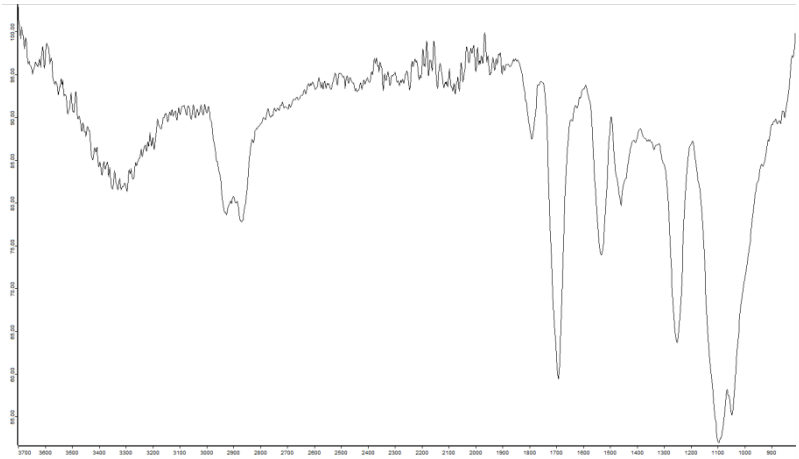

Fig. S 30 IR spectrum of NIPU sample PGC+HMDA+50 wt.-% TMPG-AA (cured at 80 °C for 14 h and post-cured 4 h at 100 °C).

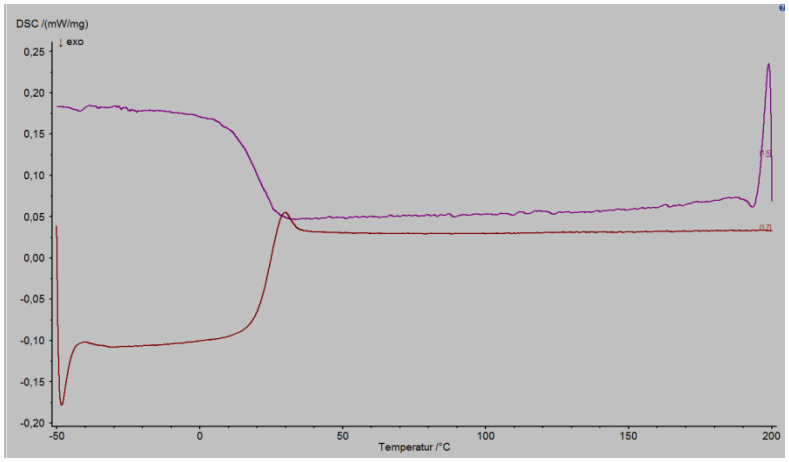

Fig. S 31 DSC measurement of GG-AA (cooling and heating rate: 10 K min^{-1}, first cooling and second heating sequence).

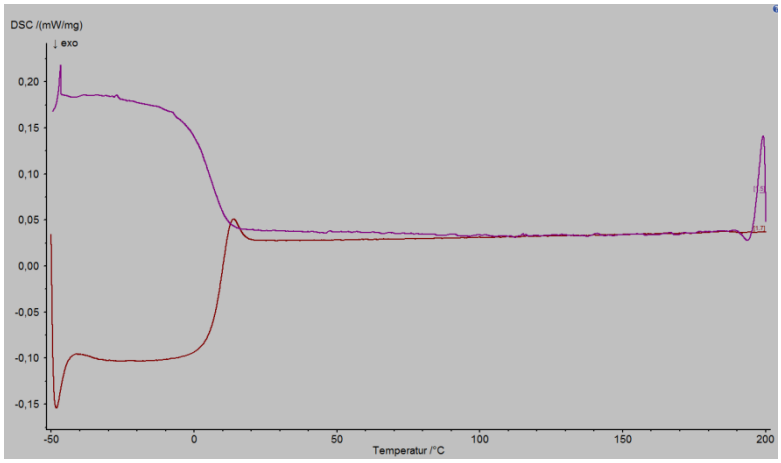

Fig. S 32 DSC measurement of TMPG-AA (cooling and heating rate: 10 K min^{-1}, first cooling and second heating sequence).

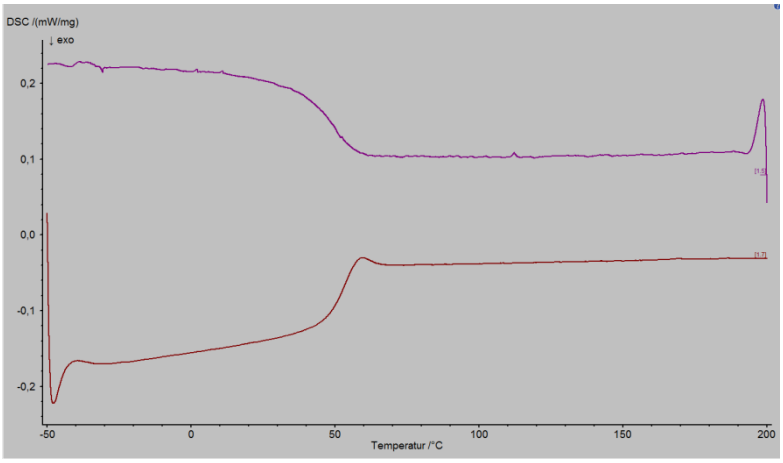

Fig. S 33 DSC measurement of PG-AA (cooling and heating rate: 10 K min^{-1}, first cooling and second heating sequence).

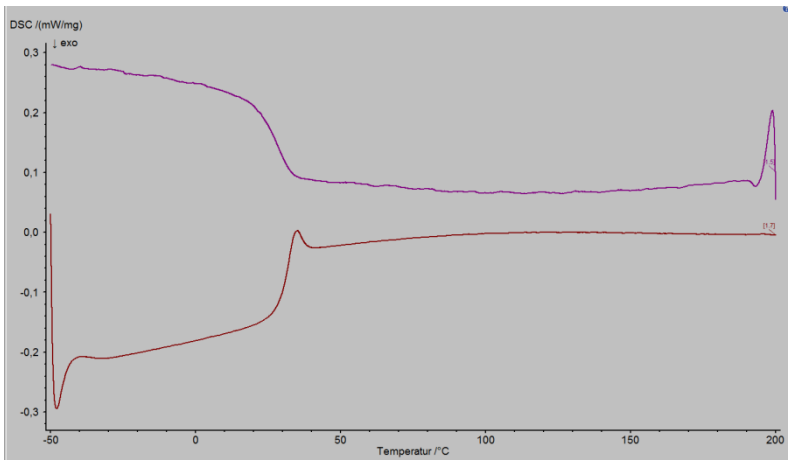

Fig. S 34 DSC measurement of crude L-AA (cooling and heating rate: 10 K min^{-1}, first cooling and second heating sequence).

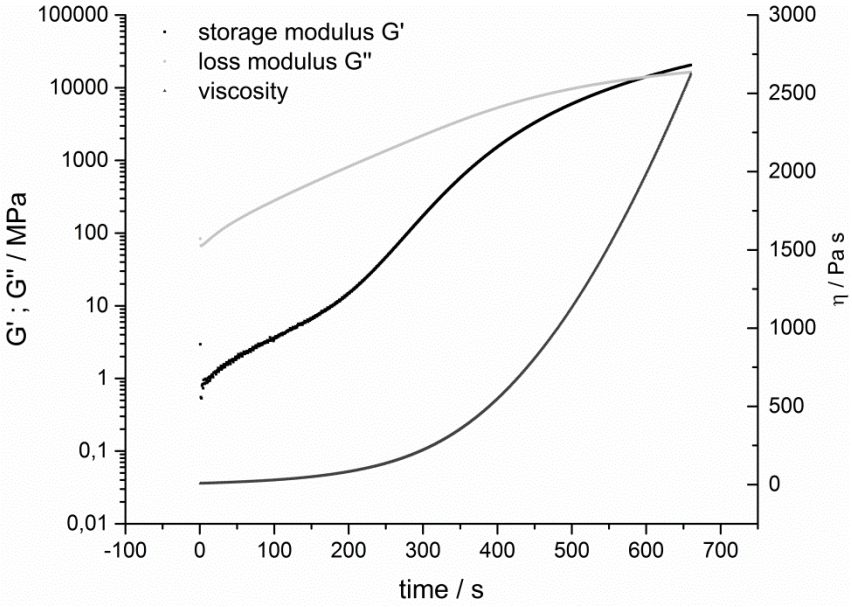

Fig. S 35 Rheological experiment for determination of gelation and pot life time at 80 °C for NIPU sample consisting of TMPGC+HMDA+ 25 wt.-% GG-AA (10 rad s^{-1}, 5 %).

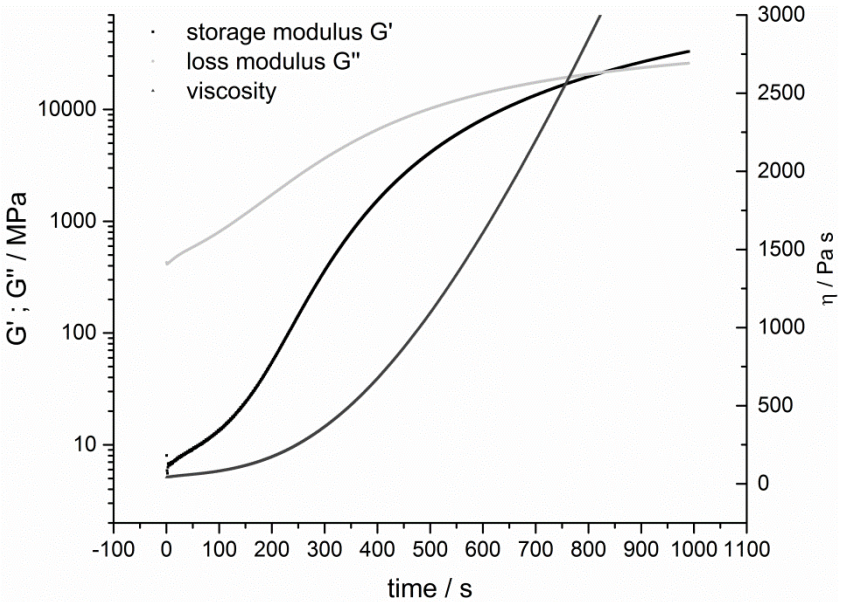

Fig. S 36 Rheological experiment for determination of gelation and pot life time at 80 °C for NIPU sample consisting of TMPGC+HMDA+ 50 wt.-% GG-AA (10 rad s^{-1}, 5 %).

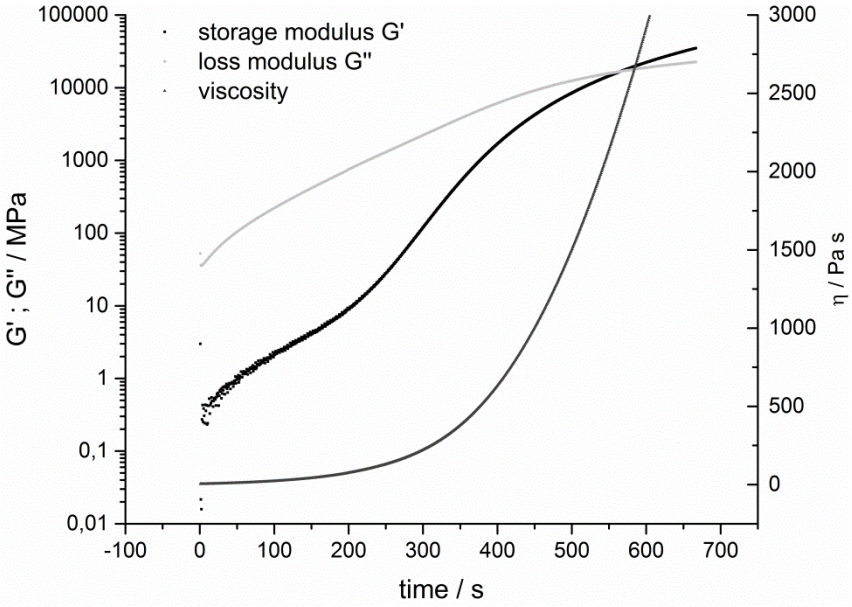

Fig. S 37 Rheological experiment for determination of gelation and pot life time at 80 °C for NIPU sample consisting of TMPGC+HMDA+ 25 wt.-% TMPG-AA (10 rad s^{-1}, 5 %).

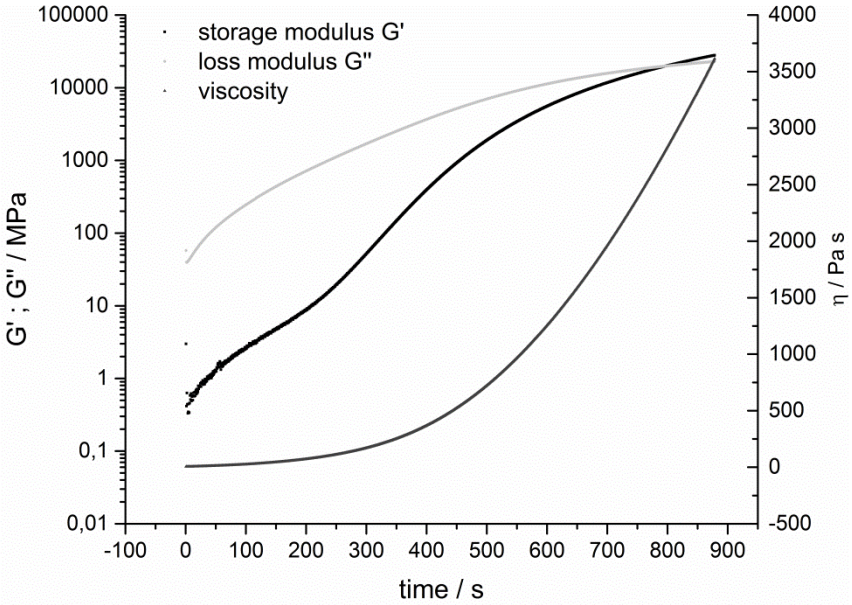

Fig. S 38 Rheological experiment for determination of gelation and pot life time at 80 °C for NIPU sample consisting of TMPGC+HMDA+ 50 wt.-% TMPG-AA (10 rad s^{-1}, 5 %).

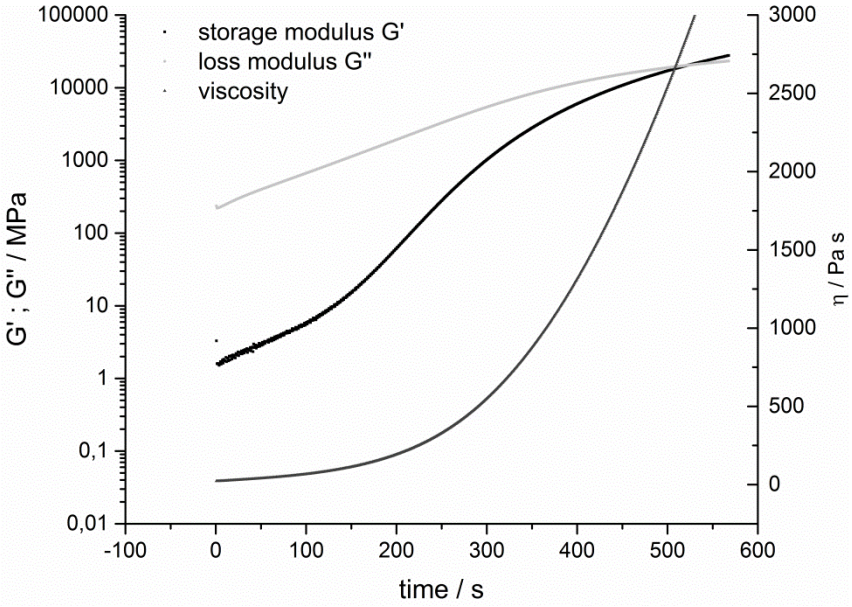

Fig. S 39 Rheological experiment for determination of gelation and pot life time at 80 °C for NIPU sample consisting of TMPGC+HMDA+ 25 wt.-% PG-AA (10 rad s^{-1}, 5 %).

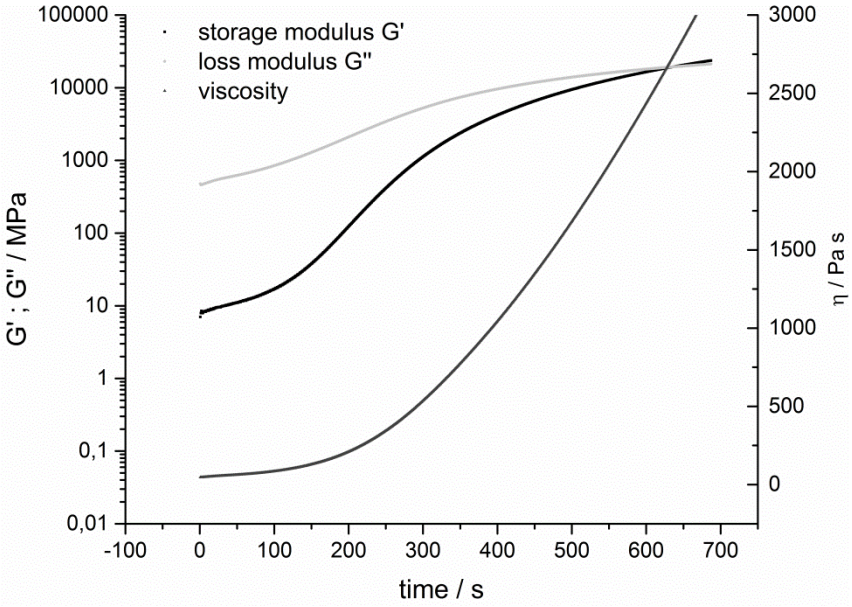

Fig. S 40 Rheological experiment for determination of gelation and pot life time at 80 °C for NIPU sample consisting of TMPGC+HMDA+ 50 wt.-% PG-AA (10 rad s^{-1}, 5 %).

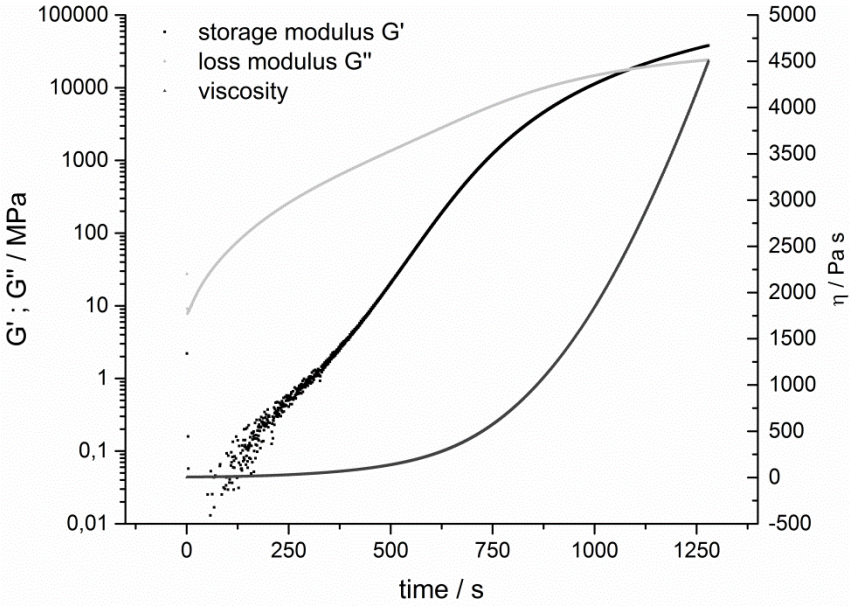

Fig. S 41 Rheological experiment for determination of gelation and pot life time at 80 °C for NIPU sample consisting of TMPGC+HMDA+ 25 wt.-% L-AA (10 rad s^{-1}, 5 %).

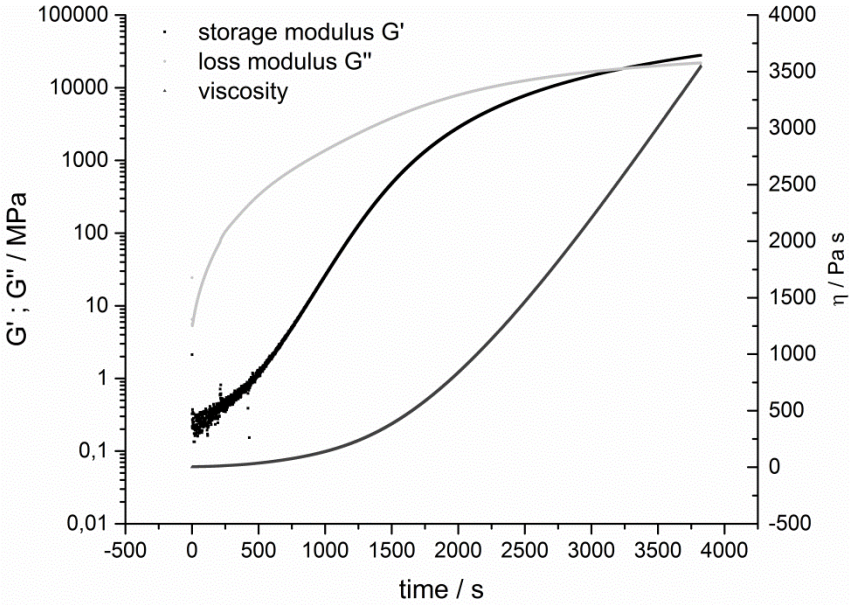

Fig. S 42 Rheological experiment for determination of gelation and pot life time at 80 °C for NIPU sample consisting of TMPGC+HMDA+ 50 wt.-% L-AA (10 rad s^{-1}, 5 %).

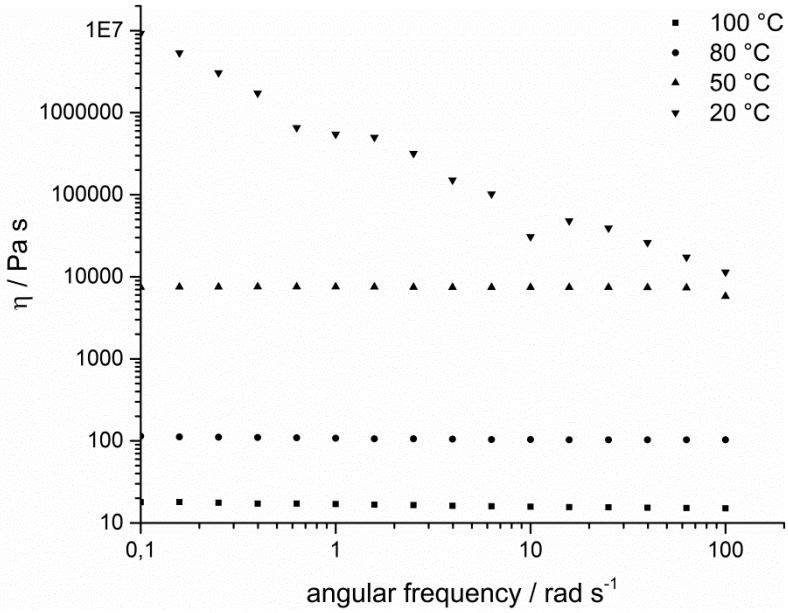

Fig. S 43 Rheological frequency sweep experiments at different temperatures for GG-AA (100-0.1 rad s^{-1}, 5 %).

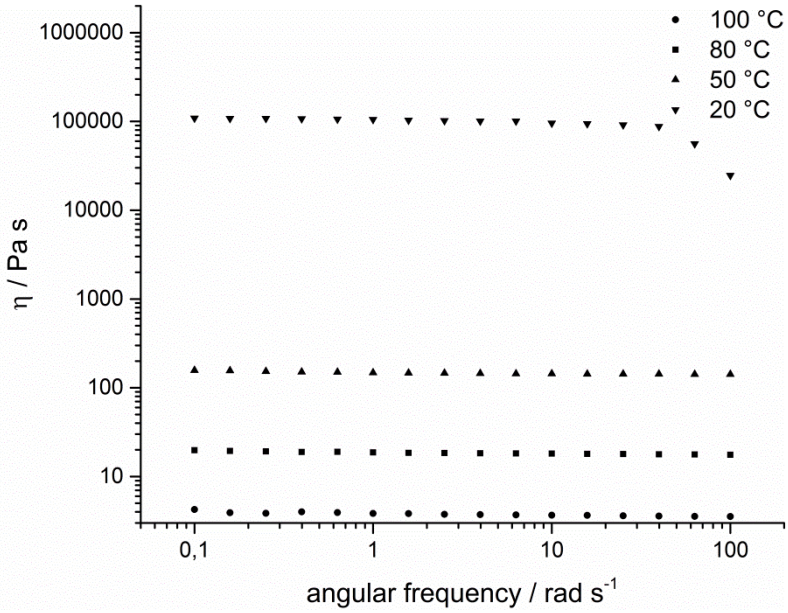

Fig. S 44 Rheological frequency sweep experiments at different temperatures for TMPG-AA (100-0.1 rad s^{-1}, 5 %).

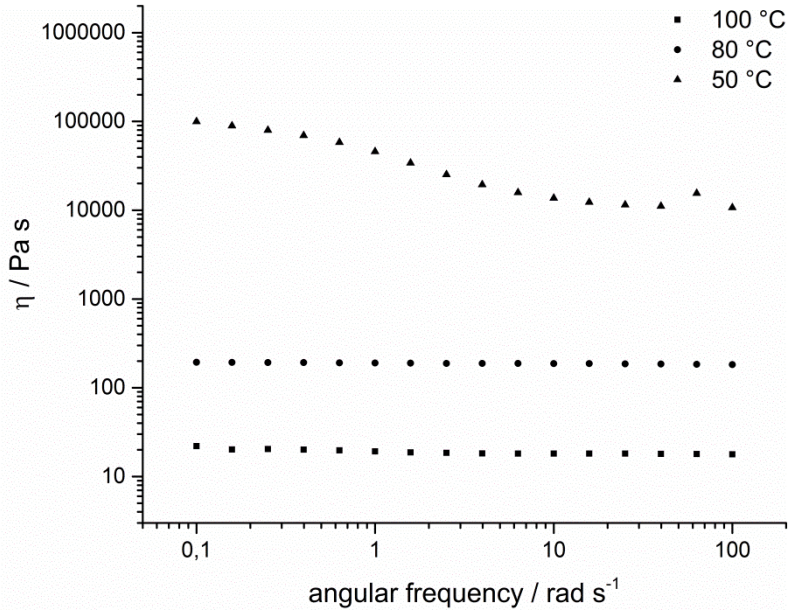

Fig. S 45 Rheological frequency sweep experiments at different temperatures for PG-AA (100-0.1 rad s^{-1}, 5 %).

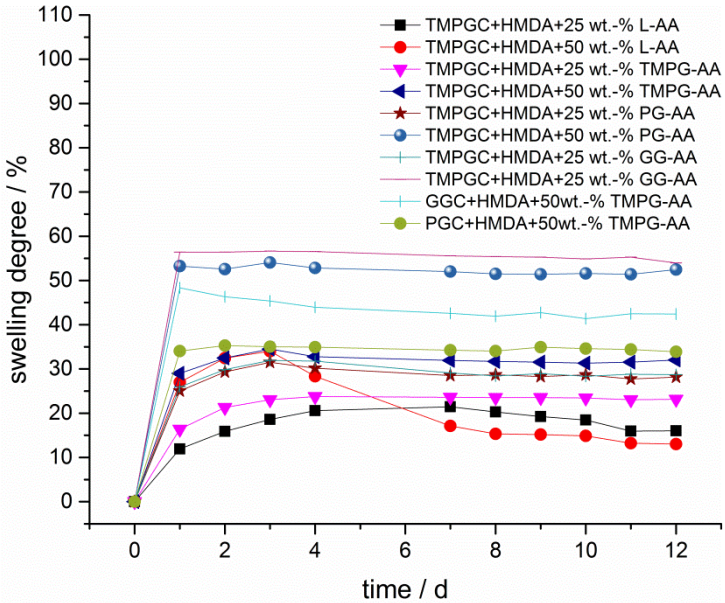

Fig. S 46 Swelling degrees in water of prepared NIPU samples.

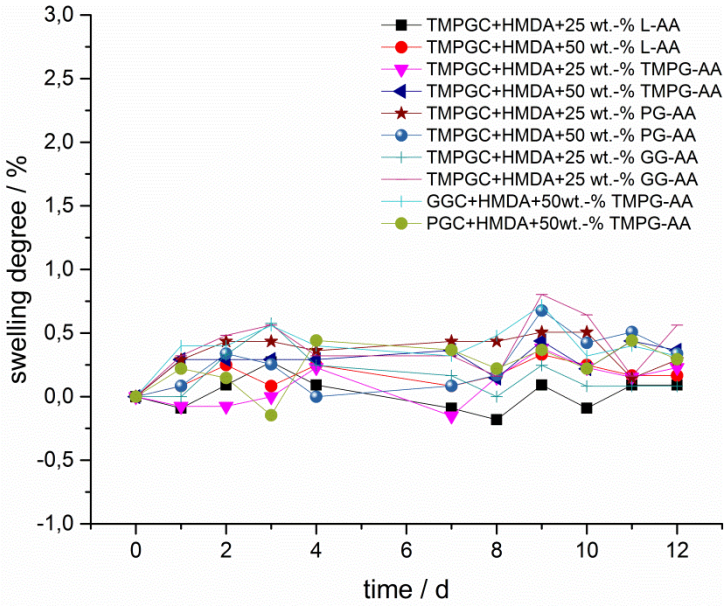

Fig. S 47 Swelling degrees in toluene of prepared NIPU samples.

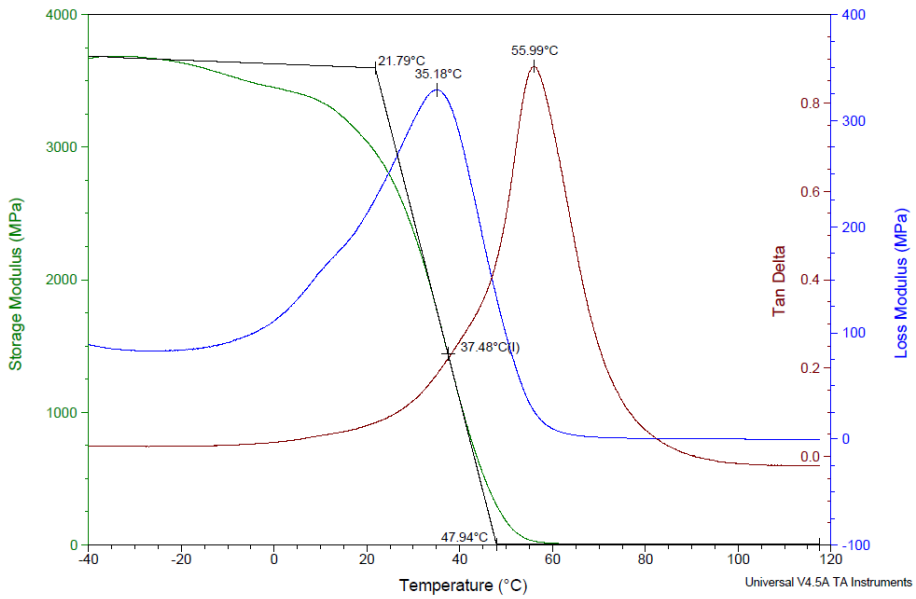

Fig. S 48 DMA curves of NIPU sample TMPGC+HMDA+25 wt.-% GG-AA (1 Hz, 0.1 %, -50-100 °C).

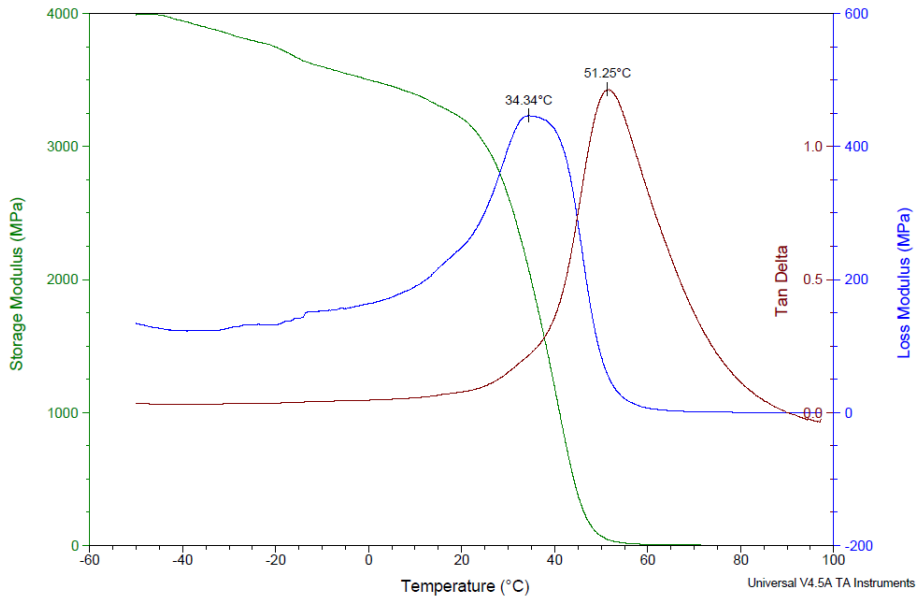

Fig. S 49 DMA curves of NIPU sample TMPGC+HMDA+50 wt.-% GG-AA (1 Hz, 0.1 %, -50-100 °C).

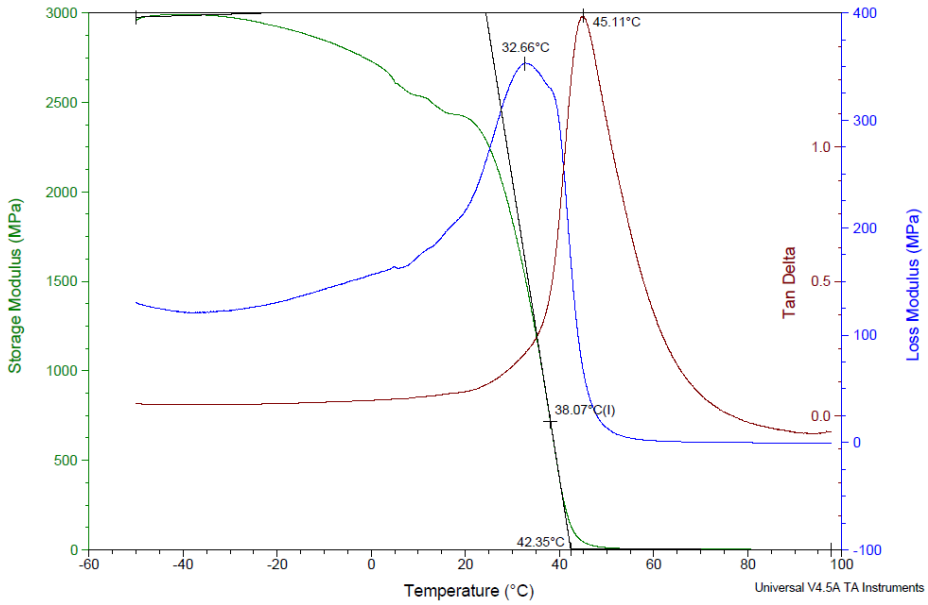

Fig. S 50 DMA curves of NIPU sample TMPGC+HMDA+25 wt.-% TMPG-AA (1 Hz, 0.1 %, -50-100 °C).

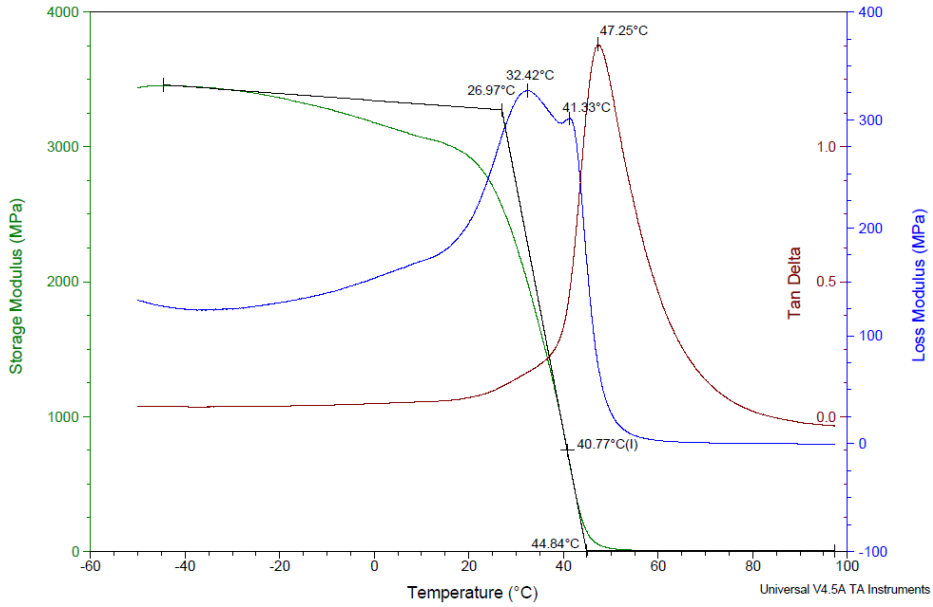

Fig. S 51 DMA curves of NIPU sample TMPGC+HMDA+50 wt.-% TMPG-AA (1 Hz, 0.1 %, -50-100 °C).

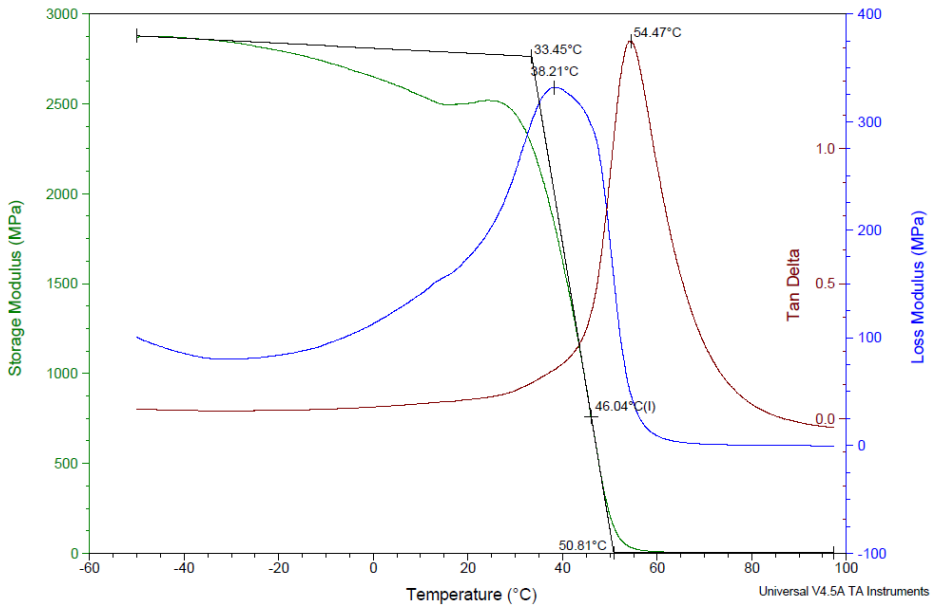

Fig. S 52 DMA curves of NIPU sample TMPGC+HMDA+25 wt.-% PG-AA (1 Hz, 0.1 %, -50-100 °C).

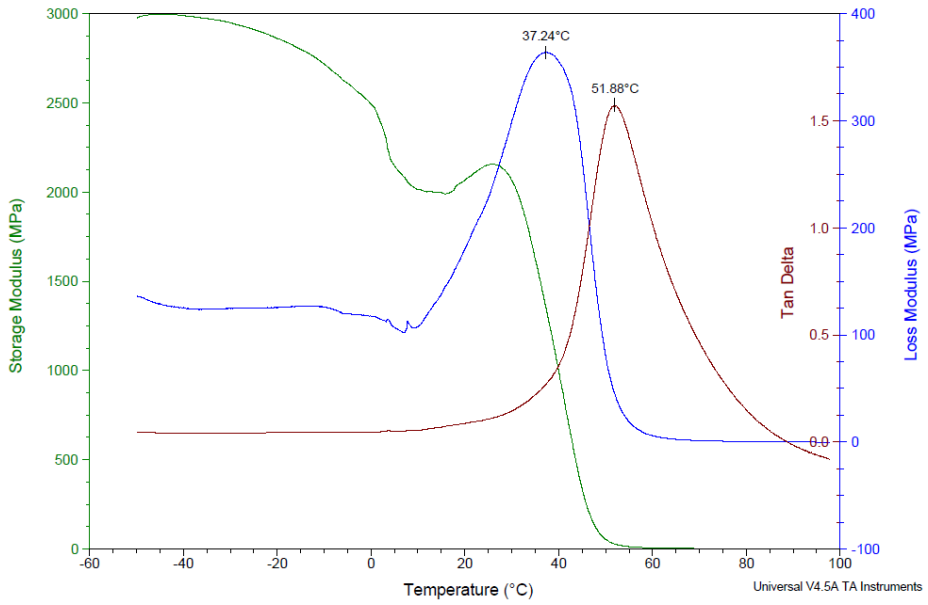

Fig. S 53 DMA curves of NIPU sample TMPGC+HMDA+50 wt.-% PG-AA (1 Hz, 0.1 %, -50-100 °C).

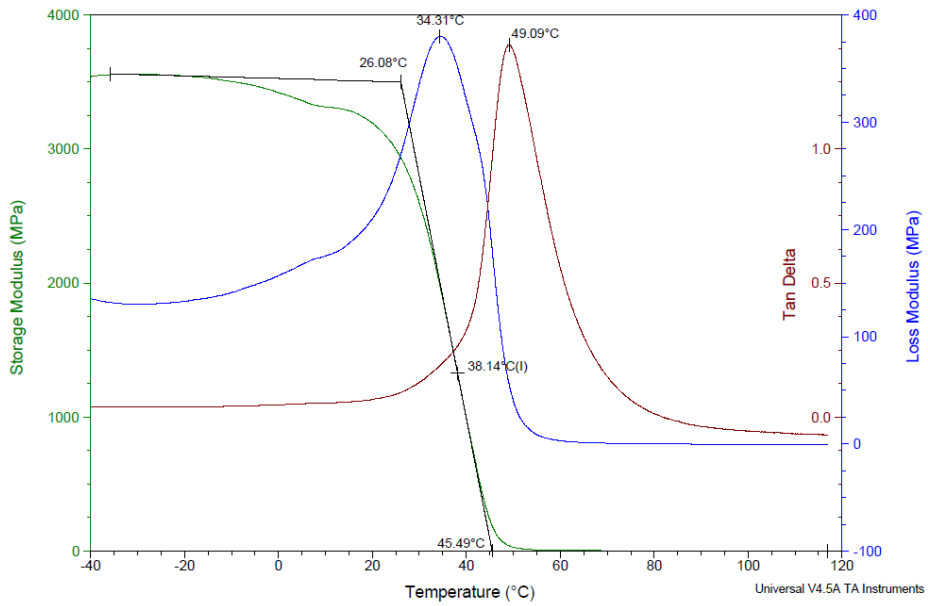

Fig. S 54 DMA curves of NIPU sample TMPGC+HMDA+25 wt.-% L-AA (1 Hz, 0.1 %, -50-100 °C).

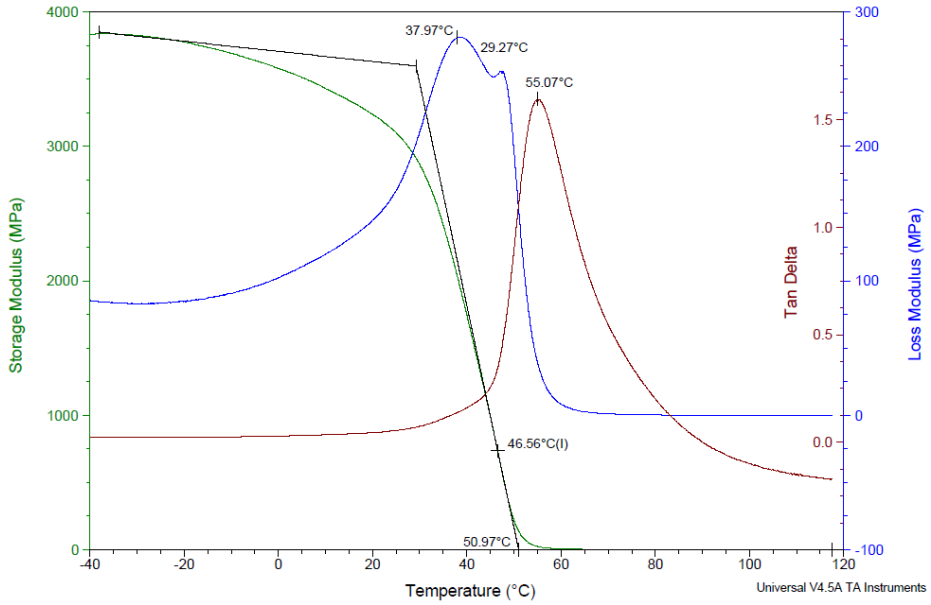

Fig. S 55 DMA curves of NIPU sample TMPGC+HMDA+50 wt.-% L-AA (1 Hz, 0.1 %, -50-100 °C).

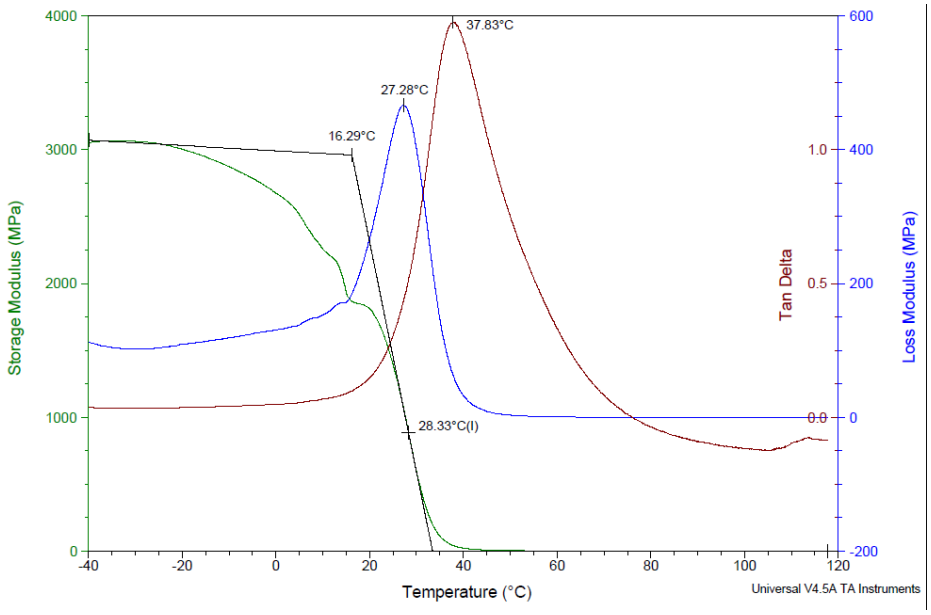

Fig. S 56 DMA curves of NIPU sample GGC+HMDA+50 wt.-% TMPG-AA (1 Hz, 0.1 %, -50-100 °C).

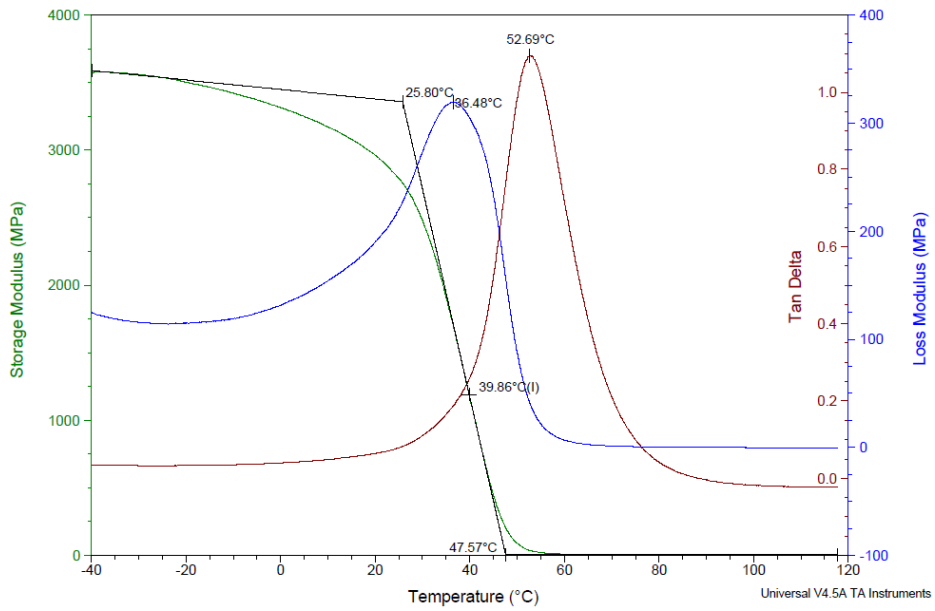

Fig. S 57 DMA curves of NIPU sample PGC+HMDA+50 wt.-% TMPG-AA (1 Hz, 0.1 %, -50-100 °C).

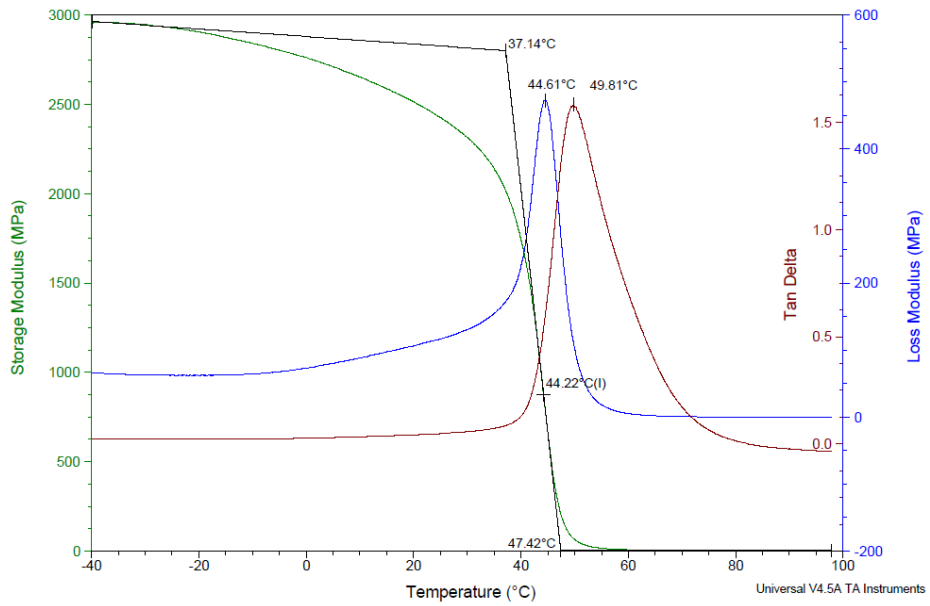

Fig. S 58 DMA curves of NIPU sample TMPGC+HMDA (1 Hz, 0.1 %, -50-100 °C).

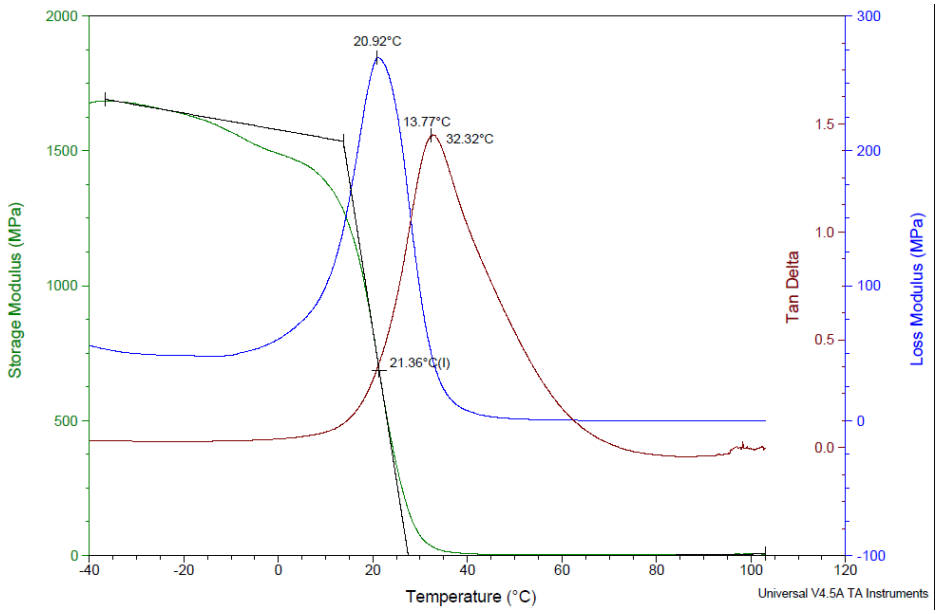

Fig. S 59 DMA curves of NIPU sample GGC+HMDA (1 Hz, 0.1 %, -50-100 °C).

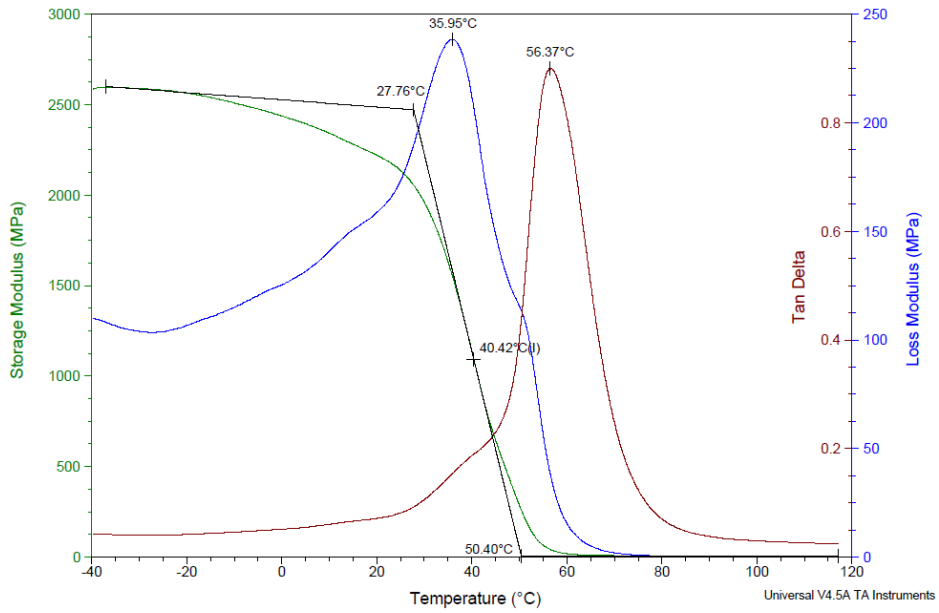

Fig. S 60 DMA curves of NIPU sample PGC+HMDA (1 Hz, 0.1 %, -50-100 °C).

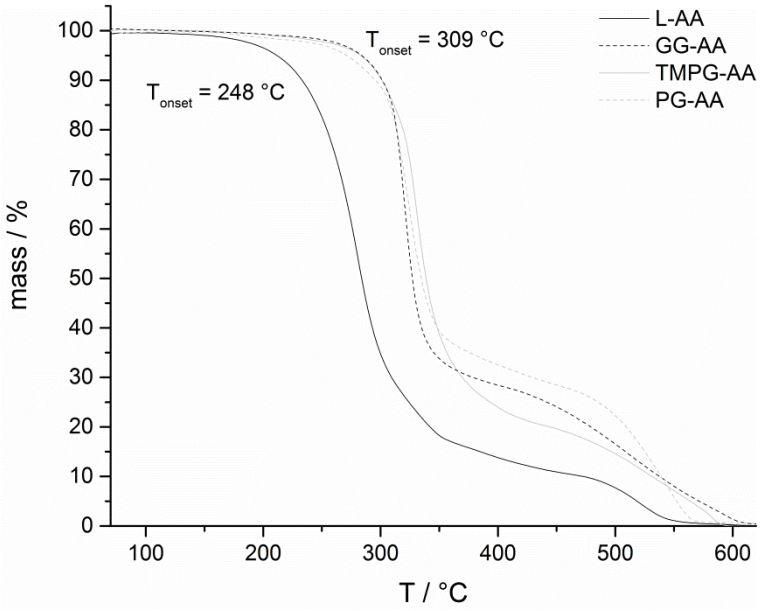

Fig. S 61 TGA curves of amino alcohols (10 K min^{-1}, air).

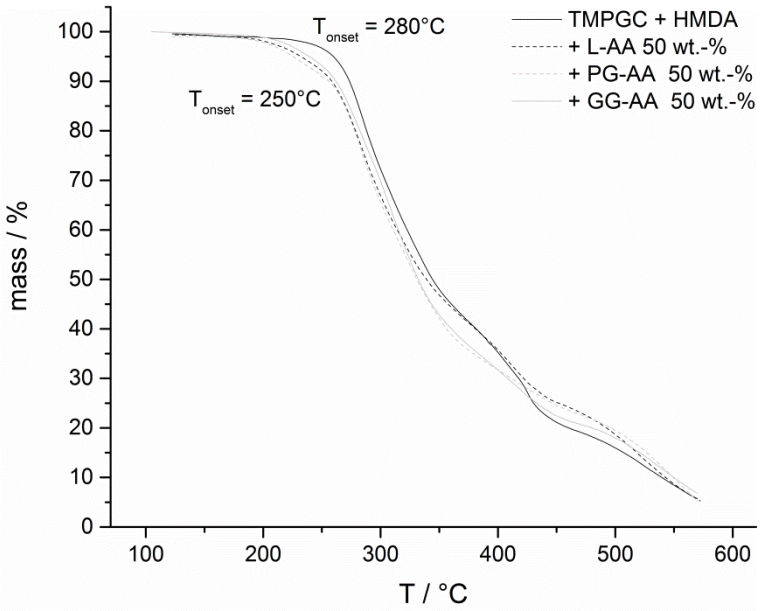

Fig. S 62 TGA curves of NIPU samples (10 K min^{-1}, air).